DEVELOPMENT OF FUNCTIONAL EMULSIONS BASED ON HUMIC ACIDS FOR COSMETIC APPLICATION

NAYRA PISCOSO SAES LOPES

Dissertation presented to the

Escola Superior de Tecnologia e Gestão – Instituto Politécnico de Bragança

to obtain the Master's Degree in

Chemical Engineering

Within the context of the double diploma with

Universidade Tecnológica Federal do Paraná

Supervisors

Prof. Dr. Maria Filomena Barreiro

Dr. Arantzazu Santamaria-Echart

Prof. Dr. Caroline Casagrande Sipoli

Prof. Dr. Bogdan Demczuk Junior

Bragança

2025

This work was supported by national funds through FCT/MCTES (PIDDAC): CIMO, UIDB/00690/2020 (DOI: 10.54499/UIDB/00690/2020) and UIDP/00690/2020 (DOI: 10.54499/UIDP/00690/2020); and SusTEC, LA/P/0007/2020 (DOI: 10.54499/LA/P/0007/2020).

"A sorte segue a coragem daqueles que enfrentam seus medos e sabem aproveitar todos os momentos."

(Mário Sérgio Cortella)

ACKNOWLEDGEMENTS

I would like to express my sincere gratitude to my advisors, Prof.ª Dr.ª Maria Filomena Barreiro and Dr.ª Arantzazu Santamaria-Echart, from the Polytechnic Institute of Bragança, as well as to Prof.ª Dr.ª Caroline Casagrande Sipoli and Prof. Dr. Bogdan Demczuk Junior, from the Federal University of Technology – Paraná (UTFPR). I am deeply thankful for their guidance, for generously sharing their knowledge, and for the wisdom they imparted throughout this journey. I am immensely grateful for their empathy, availability, constant encouragement, and for the technical and personal support I received at every stage of this work. In addition to being brilliant professionals, they are inspiring individuals whose dedication was essential to the completion of this project.

To all the professors who contributed to my academic development—from my undergraduate studies in Chemical Engineering at UTFPR to the Master's in Chemical Engineering at the Polytechnic Institute of Bragança—I offer my heartfelt thanks.

To my parents, Nivaldo Lopes da Silva and Elaine Piscoso Saes Lopes, who have always stood by my side with unwavering support and encouragement throughout my journey. To my sister, Natália Piscoso Ferraz Egreja, for her friendship and companionship. To my grandmothers, Idalina dos Anjos Piscoso Saes and Nazira Pereira da Silva, examples of strength, resilience, and wisdom—your teachings and life stories have been, and continue to be, sources of inspiration and motivation in my life. To each of you, my deepest thanks for being part of this achievement.

To my boyfriend, Guilherme Andreoli Gil, for your constant presence, unconditional love, and support throughout this journey. Your dedication, patience, and encouragement were vital every step of the way—from the long hours of thesis revisions to the emotional support that sustained me on the most difficult days. Your partnership was essential in making this dream come true. Thank you for believing in me and for walking beside me with such care, generosity, and commitment.

I would also like to express my gratitude to PhD student Giovana Colucci, whose patience and dedication were fundamental to the development of this work. I am thankful not only for her practical and intellectual support but also for her presence as a friend and solid foundation throughout this process. I am deeply grateful for her friendship, constant availability, and the care and empathy with which she accompanied me.

To my friends from UTFPR, IPB, and the laboratory, my sincere thanks for making this journey lighter and more pleasant.

ABSTRACT

The cosmetics market continues to grow, especially dermocosmetics, which combine aesthetic and therapeutic care. This growth is driving the development of more effective and sustainable formulations, such as Pickering emulsions, which utilize solid particles instead of synthetic surfactants. These latter are responsible for causing environmental impacts and adverse effects on the skin, including irritation and allergies. Humic acid, a natural active ingredient with antioxidant, anti-inflammatory, and photoprotective properties, is an innovative alternative for this type of system. In this context, this work aims to study Pickering emulsions stabilized with humic acid nanoparticles for the development of a dermocosmetic product. Different conditions for producing the particles were analyzed, including the solvent and anti-solvent used, concentration, and pH. The optimized nanoparticles were obtained by acid precipitation, using 0.5 M sodium hydroxide to solubilize the humic acid (final concentration of 10 g/L) and 0.5 M citric acid as the precipitating agent. The optimized particles were used to formulate Pickering emulsions, with an oil volume percentage of 65% showing the best results. The humic acid particles had an average particle size of 73.9 ± 9.7 nm and a three-phase contact angle (particles-water-sweet almond oil) of 65 ± 3.5º, revealing a hydrophilic character. The optimized emulsion consisted of round-shaped droplets with an average size of 44.2 ± 0.3 μm, resulting in an emulsified layer of over 95%, which indicated high stability after 30 days of storage. In addition, the emulsion exhibited a brown color, 14.8% inhibition of antioxidant activity, and, according to rheological analysis, a pseudoplastic, non-Newtonian fluid behavior with gel-like characteristics. It had a smooth texture to the touch, was easy to spread, and had low tackiness. These results demonstrate not only the feasibility of using humic acid particles as stabilizers in Pickering emulsions but also highlight their multifunctional potential for cosmetic applications. This is an unprecedented approach in the field of dermocosmetics, with scientific and technological relevance. Overall, this study presents an innovative, ecological, and effective alternative to the use of synthetic surfactants, offering new perspectives for the development of sustainable cosmetic products based on physical stabilization technologies utilizing nanoparticles.

Palavras-chave: humic acid; nanoparticles; Pickering emulsions; dermocosmetics.

RESUMO

O mercado de cosméticos segue em ascensão, com destaque para os dermocosméticos, que aliam cuidados estéticos e terapêuticos. Esse crescimento impulsiona o desenvolvimento de formulações mais eficazes e sustentáveis, como as emulsões Pickering, que utilizam partículas sólidas como substitutos de surfactantes sintéticos. Estes últimos são responsáveis por causarem impactos ambientais e efeitos adversos na pele, como irritações e alergias. O ácido húmico, um ativo natural com propriedades antioxidantes, anti-inflamatórias e fotoprotetoras, surge como uma alternativa inovadora para esse tipo de sistema. Neste contexto, o objetivo deste trabalho consistiu no estudo de emulsões Pickering estabilizadas com nanopartículas de ácido húmico para o desenvolvimento de um produto dermocosmético. Foram estudadas diferentes condições para a produção das partículas, incluindo o tipo de solvente e o anti-solvente utilizados, concentração e pH. As nanopartículas otimizadas foram obtidas por precipitação ácida, utilizando-se hidróxido de sódio 0.5 M para solubilização do ácido húmico (concentração final de 10 g/L) e ácido cítrico 0.5 M como agente precipitante. As partículas otimizadas foram utilizadas na formulação de emulsões Pickering, sendo a proporção óleo/água de 65/35 a que apresentou os melhores resultados. As partículas de ácido húmico apresentaram tamanho médio de partícula de 73.9 ± 9.7 nm e ângulo de contato trifásico (partículas-água-óleo de amêndoas doces) de 65 ± 3.5º, revelando um caráter hidrofílico. A emulsão otimizada apresentou gotículas de formato arredondado de tamanho médio de 44.2 ± 0.3 μm, e uma camada emulsionada superior a 95%, indicando uma estabilidade elevada após 30 dias de armazenamento. Adicionalmente, a emulsão apresentou coloração castanha, 14.8% de inibição de atividade antioxidante e, de acordo com a análise reológica, um comportamento de fluido não-Newtoniano pseudoplástico, com características semelhantes a um gel. Apresenta uma textura suave ao toque, de fácil espalhamento e com baixa pegajosidade.

Esses resultados demonstram não apenas a viabilidade do uso de partículas de ácido húmico como estabilizantes em emulsões Pickering, mas também destacam seu potencial multifuncional para aplicações cosméticas. Trata-se de uma abordagem inédita no campo da dermocosmética, com relevância científica e tecnológica. Em síntese, o presente estudo contribui com uma alternativa inovadora, ecológica e eficaz ao uso de surfactantes sintéticos, abrindo novas perspectivas para o desenvolvimento de produtos cosméticos sustentáveis baseados em tecnologias de estabilização física por nanopartículas.

Palavras-chave: ácido húmico; nanopartículas; emulsões Pickering; dermocosméticos.

INDEX

INDEX OF FIGURES

INDEX OF TABLES

INDEX OF SYMBOLS

EII	Emulsion Instability Index
EL	Emulsified Layer
HA	Humic acid
HA-P	Humic acid particles
HSs	Humic substance
LVR	Linear Viscoelastic Region
O/W	Oil in water
O/W/O	Oil in water in oil
SAPMENA-SSA	South Asia Pacific, Middle East, North Africa, Sub-Saharan Africa
SDG	Sustainable Development Goals
TEM	Transmission electron microscopy
UN	United Nations
UV	Ultraviolet radiation
W/O	Water in oil
W/O/W	Water in oil water

1. Motivation and objectives

According to McKinsey & Company (2023), the beauty industry generated approximately $430 billion in revenue in 2022, with steady growth over the years (Figure 1). Following the recovery from the COVID-19 pandemic, which led to an 8% decline in the sector, the beauty market is projected to grow 6% annually, reaching approximately $580 billion by 2027, highlighting the sector's resilience and long-term growth potential [1,2].

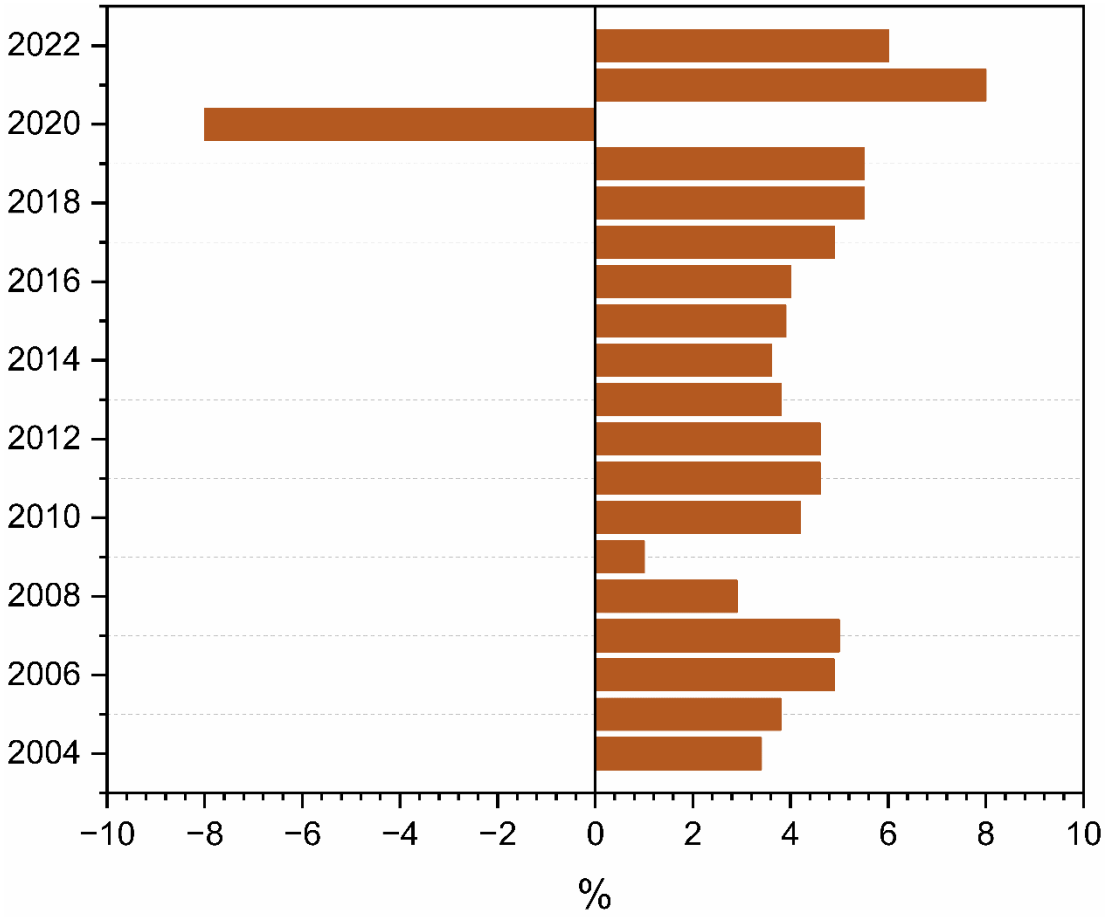

Figure 1 - Annual growth rate of the cosmetics sector in the world from 2004 to 2022.
Source: adapted from L'Oreal [2].

As shown in Figure 2 [2,3], Asia is the geographical region with the highest consumption in the global cosmetic market in 2022, accounting for 32% of this market. It is followed by North America (28%), Europe (22%), South Asia Pacific, Middle East, North and Sub-Saharan Africa (SAPMENA-SSA) (10%), and Latin America (8%).

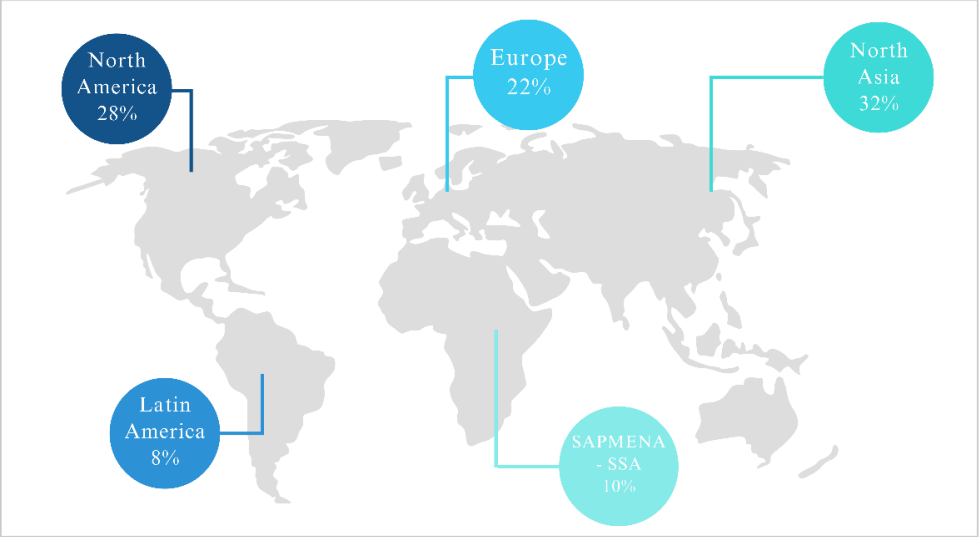

Figure 2 - The global estimated cosmetic market in 2022.
Source: adapted from L'Oreal [2].

Increased awareness of skin and hair care is a growth factor in the cosmetics and dermocosmetics market. Dermocosmetics enhance the skin's appearance and address skin disorders, including wrinkles, acne, blemishes, and signs of aging. The global market trend of dermocosmetics is to achieve 90.8 billion dollars by 2028, showing a rising market.

The cosmetics sector will need to undergo significant transformation to adapt to the expanding diversity of products, distribution channels, and markets by the end of this decade. This evolution will be driven primarily by consumers, particularly younger generations, whose evolving definitions of beauty, shifting views on sustainability, and changing attitudes toward influencers are reshaping the industry landscape [1].

It is known that natural and organic products are gaining increasing popularity, especially among the younger generations. Thus, there are increasing studies and research on assets to meet consumer expectations [4]. In this context, there is a growing scientific interest in new active ingredients and technologies that meet the expectations of a changing market. Emulsions, widely used products in the cosmetics industry, play a crucial role due to their ability to combine hydrophilic and lipophilic ingredients, thereby enabling the effective delivery of bioactive compounds to the skin. However, conventional emulsions typically rely on synthetic surfactants for stabilization, which can trigger adverse skin reactions and pose environmental risks.

Given these limitations, Pickering emulsions have emerged as an innovative alternative. In this type of system, stabilization occurs through solid particles adsorbed on the oil-water interface, providing greater physical stability, lower toxicity, and better

biocompatibility, in line with the principles of sustainability. By combining technological innovation with environmental responsibility, Pickering emulsions have emerged as a promising strategy for cosmetic applications. This growing interest is reflected in the significant increase in scientific research: between 2000 and 2024, there was a substantial increase in scientific publications on the topic. In the last year, the number of papers on “Pickering Emulsions” grew by around 37%. In comparison, specific publications on Pickering emulsions in the cosmetics area showed an increase of approximately 32%, as illustrated in Figure 3.

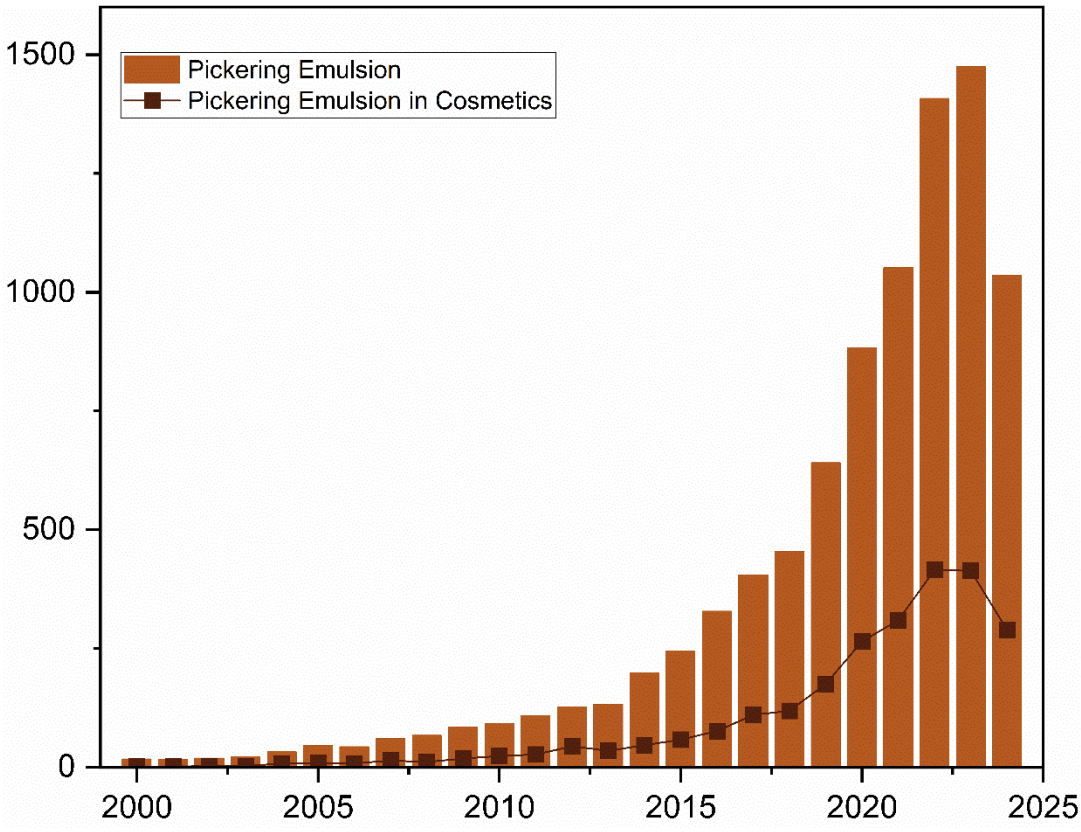

Figure 3 - Articles related to the term Pickering emulsions (considering all application types) and Pickering emulsions applied in cosmetics from 2000 to 2024.
Source: adapted from Science Direct.

The increased use of Pickering emulsions can be attributed to their greater stability compared to conventional emulsions, as well as their enhanced biological compatibility, low cost, low toxicity, and broad applicability [5–7]. Thus, Pickering emulsions offer several advantages for designing innovative and sustainable cosmetic products.

Finding innovative, sustainable, and biocompatible materials to act as stabilizing particles in Pickering emulsions represents a significant challenge in the development of cosmetic formulations. The growing demand for natural and functional ingredients drives the

search for alternatives to conventional stabilizers, which are often synthetic and potentially irritating. In this context, humic acid has emerged as a promising solution. It is an organic compound of natural origin with bioactive properties, including antioxidant activity, stimulation of collagen synthesis, tissue regeneration, and protection against UV-B radiation. These characteristics make humic acid a promising option for dermocosmetic applications, both due to its therapeutic potential and its ability to stabilize emulsions through the Pickering mechanism [8].

This new formulation can promote consumer benefits and bring innovation to the sector, aligning with some of the Sustainable Development Goals (SDGs) established by the United Nations (UN) (Figure 4). These include SDG 3, related to promoting well-being and healthy lives for all ages by offering a safer dermocosmetic alternative that promotes health and wellness. It relates to SDG 9 by encouraging scientific research and innovation in the cosmetics area through the use of sustainable technologies based on natural materials. It also supports SDG 12 by proposing a solution based on a natural compound, promoting cleaner, safer, and more environmentally responsible production practices with lower impact throughout the product's life cycle.

Figure 4 - Sustainable Development Goals 3, 9, and 12.
Source: United Nations Organization (UN).

1.1. General objective

This study examines the application of humic acid nanoparticles as stabilizing agents in Pickering emulsions, with a focus on their potential cosmetic applications.

1.2. Specific objectives

1) To explore the production of humic acid nanoparticles using the acid precipitation method under different process conditions, such as solvent type and humic acid concentration;
2) To characterize the particles obtained in terms of size, zeta potential, morphology, wettability, and emulsifying potential;
3) To develop and optimize Pickering emulsion formulations by evaluating processing variables such as particle concentration, type of oil phase, and water/oil ratio;
4) To characterize the emulsions in terms of morphology, size, emulsified layer, texture, color, and antioxidant activity.

To address Objective 1, Section 3.4 describes the methodology used for the production of humic acid particles, while Section 4.3 discusses the effect of pH on this process and Section 4.4 examines the influence of the acidic precipitating agent and humic acid concentration Regarding Objective 2, Sections 3.6.1, 3.6.2, 3.6.3 describe the methodologies for analyzing zeta potential and particle size, morphology, and wettability, respectively, with the results discussed in Section 4.5. For the emulsions, Section 3.5 details the preparation procedure, while Sections 4.6 e 4.7 describe the particle stabilization mechanism within the emulsion and the effect of oil volume fraction in the system, addressing Objective 3. Finally, to achieve Objective 4, Sections 3.6.2, 3.6.5, 3.6.6, 3.6.7, 3.6.8, 3.6.9 and 3.6.10 describe the methodologies used in the analyses of morphology, droplet size, stability, antioxidant activity, rheological properties, texture, and color of the emulsions, with the corresponding results discussed in Section 4.8.

2. Literature review

This section is dedicated to the literature review, contextualizing the theme through the approach of subjects such as the cosmetic industry, dermocosmetics, skin and culture permeation, conventional emulsions, Pickering emulsions, the application of Pickering emulsions in the cosmetic industry, solid particles, humic acid (HA) and acid precipitation method for particle synthesis.

2.1. Cosmetic industry

The word "cosmetics", from the Greek *kosmétikos*, is the set of activities, products, or services that aim to protect or improve the appearance and odor of the human body. It includes makeup products, skincare, perfumes, toiletries, and services associated with beauty salons [3,4].

The history of cosmetics dates back to ancient Egyptian civilization. It is believed that the use of oils, perfumes, and makeup was not only for aesthetic purposes but also for protection from arid climates and high temperatures; therefore, they were associated with healthcare.

The growth of the beauty market was closely interconnected with globalization and the mass production of cosmetics in the twentieth century [3,9]. At the end of the twentieth century, with the substantial advancement of innovation, cosmetics ceased to be merely aesthetic products, beginning to be considered therapeutic products, such as anti-aging, anti-dark spots, and anti-acne treatments.

The global cosmetics market is dynamic and powerful, influenced by habits and economic factors. Consumption is sustained mainly by the expansion of social networks and consumer interest in new products. Its main characteristic is that it is continuously researched, which generates constant innovation in products [3].

Consumers demand better and safer products and decide the path of innovation. However, these requirements change rapidly, forcing the market to be increasingly dynamic. To maintain customer satisfaction, aspects such as quality, performance, and the adoption of new technologies must be prioritized [3].

2.2. Dermocosmetics

Dermocosmetics is a branch of dermatology that uses cosmetics with active ingredients to treat skin disorders. Thus, dermocosmetic products used alone or as adjuncts to pharmacological treatment, are applied to penetrate the stratum corneum to provide certain

benefits such as improving photoprotection, dry or aging skin, skin diseases (acne, rosacea, psoriasis, atopic dermatitis, and seborrheic dermatitis), as well as a variety of hair and nail disorders [9–11].

The Food, Medicines, and Cosmetics Act of 1938 defines cosmetics as products intended to cleanse, care for, beautify, and improve the appearance of the skin, and medicines as products intended to affect the structure or any function of the body, in addition to the treatment or prevention of disease [12]. Thus, dermocosmetics were developed to bridge the gap between cosmetics and pharmaceuticals. They achieve a cosmetic effect through active substances, but they are not subject to drug regulation.

The term "dermocosmetics" was first used by Raymond Reed to describe formulations for the care and treatment of dermatological diseases. In 1974, this term was popularized by Albert Kligman, who emphasized that it was a new group of formulations that combined the characteristics of a drug and a cosmetic. However, despite this term being more than 40 years old, it has yet to be recognized by the regulations of the Food and Drug Administration (FDA) in the United States (USA) and regulatory agencies in the European Union [12].

The formulations of dermocosmetics can be creams, ointments, gels, serums, bath oils, or micellar water. The formulation can contain several active principles such as vitamins, antioxidants, hyaluronic acid, salicylic acid, retinoids, peptides, and plant extract, among others [10,12]. The optimal skincare regimen for a particular patient will depend on factors such as age, sex, skin type, and underlying conditions, as well as exposure to external factors like sun exposure, pollution, and temperature. In addition, it also depends on aspects related to lifestyle, such as stress, lack of sleep, poor nutrition, smoking, and hormonal dysregulation [11].

2.3. Skin and skin permeation

The development of the cosmetic industry is based on a deep understanding of skin structures and their functions. The skin is considered the largest organ of the human body. It constitutes a protective barrier for the human body against external environmental aggressions, such as pathogens, solar radiation, chemical agents, and mechanical lesions [4,13]. In addition, the skin can vary in thickness and pH depending on the body region [14].

In addition to acting as a physical barrier, the skin serves other vital functions, including regulating body temperature, preventing and controlling water loss, and participating in the excretion process through sweat. It is also the primary organ synthesizer of vitamin D3 of the organism and produces melanin for protection against solar radiation [4,13,14].

The skin consists of three main layers: the epidermis, dermis, and hypodermis. The epidermis is the outermost layer of the skin, followed by the dermis, and the innermost is the hypodermis (Figure 5).

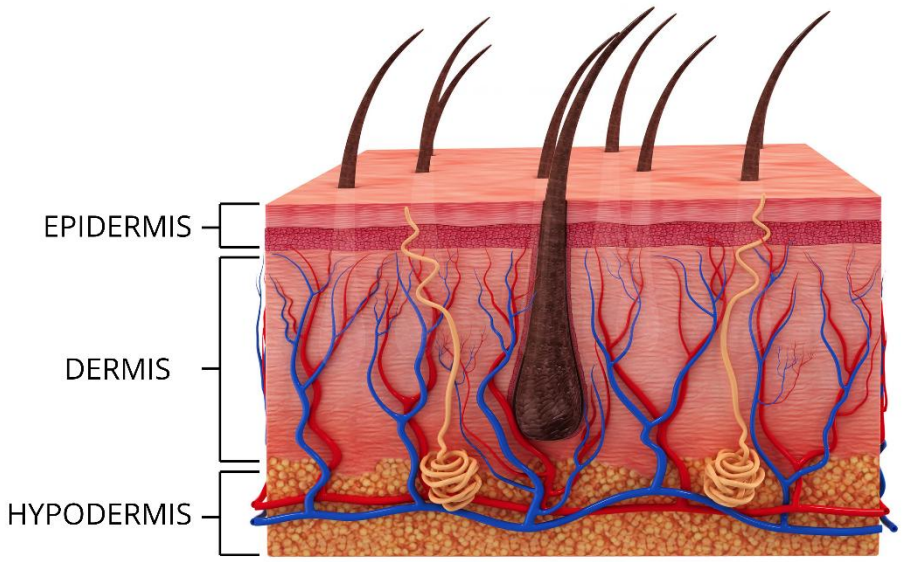

Figure 5 - Illustration of the skin and its layers.
Source: adapted from Alves N. C. [13]

The epidermis is the outermost layer and the most active layer since it is constantly renewed. On its outer surface is the stratum corneum, which serves as the primary barrier preventing the permeation of drugs and cosmetics through the skin [4,14,15].

The dermis is the middle support layer located below the epidermis. It provides mechanical strength, firmness, and elasticity to the skin [4,14,15]. Collagen is the primary component of the dermis, a fibrous protein that helps resist mechanical abrasion and maintain tissue structure [14,16].

The hypodermis, the deeper layer, forms layers of fatty tissue that isolate and protect the skin. The hypodermis is important in endocrine function and secretes stimulating factors that play essential roles in lipid metabolism, energy balance, insulin sensitivity, immunomodulation, and inflammatory response [4].

Numerous factors can cause changes in the three layers of the skin, affecting skin health and generating aesthetic changes. Climatic factors, such as increased sweating, pathologies, and reduced water intake, are mainly responsible for the imbalance of the corneal layer, which maintains the skin's hydration level [15].

Regardless of the skin type, hydration is essential to restoring the skin's natural layer of protection. Without it, water loss will be greater and tissue oxidation lower, resulting in dehydration of the skin surface, making the skin dull and rough and favoring the appearance of wrinkles [15].

Several active ingredients are added to cosmetics, which differ in their affinity and act on several fronts, such as antioxidant defense, stimulation of cell renewal, synthesis of collagen and elastin, and promotion of hydration, all to maintain the appearance of healthy and young skin. However, to have results, the permeation of a cosmetic's active ingredients must happen [15].

Penetration occurs when the active passes only through the stratum corneum, while permeation occurs when the active passes through the epidermis and reaches the dermis. Skin penetration and absorption describe active ingredients that act topically, such as cosmetic and dermatological formulations. However, skin permeation or transcutaneous absorption refers to formulations with systemic action that act by the transdermal route [13].

There are three ways for an asset to traverse the stratum corneum: intercellular, transcellular, and appendages. The active ingredient diffuses into the stratum corneum through the intercellular route, passing between the cells. Through the transcellular pathway, the active directly crosses the cells and the lipid matrix. And via appendages, the active is absorbed by the sebaceous glands, sweat, and hair follicles [13,14].

The most common form of skin permeation is the intercellular pathway. The transcellular pathway requires the overcoming of many layers of cells, which makes the active penetration difficult, and the appendix pathway is limited to the application of the product at the exact site [14].

However, the skin has a natural property that, according to its needs, the tissue accepts the permeation of the actives according to its physiological nature and its physicochemical characteristics, defining selective cell permeability. Among the physicochemical characteristics that stand out are polar character, electric charge, concentration, temperature, pH, biocompatibility, and the need for the active to be slightly lipophilic [15].

Studies report that skin penetration is interesting when substances with solubilization properties in water and lipids are used. In this way, emulsions are a great vehicle for the actives to reach the desired layer [13].

2.4. Conventional emulsions

For a long time, the best-known applications of emulsions were in the food industry, using animal products such as egg yolk lecithin and milk proteins, mainly used in the preparation of mayonnaise, seasonings, and desserts [17]. Currently, emulsions are used in various areas of industry, such as the production of pharmaceuticals, personal care, paints, food, and cosmetics [6,7,17–19].

Emulsions are defined as heterogeneous systems formed by two or more liquids, in which one of them is dispersed in the form of droplets (dispersed phase) in another (continuous phase) [6,7,20]. The basic components of an emulsion are the aqueous phase and the oily phase, and the more polar liquid is represented by the aqueous phase and the less polar liquid by the oily phase [21].

Emulsions can be classified according to the dispersed phase, being oil dispersed in water (O/W) or water dispersed in oil (W/O) (Figure 6) [21,22]. In addition, there are multiple emulsions, with O/W/O and W/O/W systems, which are less used due to high complexity and instability [21].

In the cosmetic industry, O/W emulsions have lighter sensory aspects, with better spreadability, freshness, and lightness. In addition, they provide less occlusion to the skin because the dispersant medium is aqueous [21,22]. W/O emulsions form a coating film on the skin and tend to be waterproof. These have an occlusive effect and can lead to the formation of sebaceous comedones. Therefore, O/W emulsions are the most used type of emulsion system in the cosmetic industry [21,22].

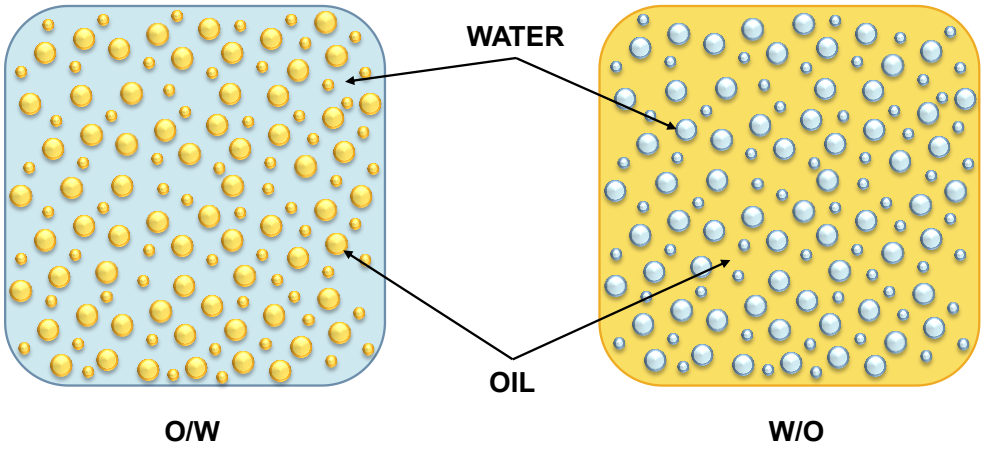

Figure 6 - Types of emulsions.
Source: adapted from Fidelis L. [21].

For the dispersion and formation of an emulsion, it is necessary to break the dispersed phase into smaller droplets using some stirring [20,22]. The duration of the stirring step greatly influences the emulsification process because, with prolonged stirring, there is a greater probability of collision between the droplets and coalescence, and a decrease in the viscosity may occur [21]. Thus, the degree of stirring required will depend on the total volume of liquid, viscosity, and surface tension at the oil/water interface in the system [20,21].

Conventional emulsions are thermodynamically unstable; that is, they destabilize over time and can undergo phase separation through different mechanisms (Figure 7):

1. *Phase inversion:* occurs when a W/O emulsion turns into an O/W or vice versa [23,24].
2. *Creaming and sedimentation*: occur due to the differences in density between the phases. The droplets aggregate in the continuous phase, generating an oily layer on the surface (creaming) or bottom (sedimentation). These aggregation processes can be reversed by agitation. However, emulsion breakage may occur in extreme cases due to gravitational separation [23,24].
3. *Flocculation:* a process that occurs between two or more droplets that aggregate and form flakes. However, stirring can easily reverse it because this aggregation happens by Van der Waals forces, which are low intensity [23,24].
4. *Coalescence*: follows a physical process of subsequent aggregation to flocculation, in which small droplets merge to form larger ones. This process is irreversible and leads to the breakdown of the emulsion [23,24].
5. *Ostwald ripening:* is a mechanism related to the diffusion of the dispersed phase through the continuous phase due to the partial solubility between the phases. Thus, it contributes to the growth of droplets with greater area and volume [23,24].

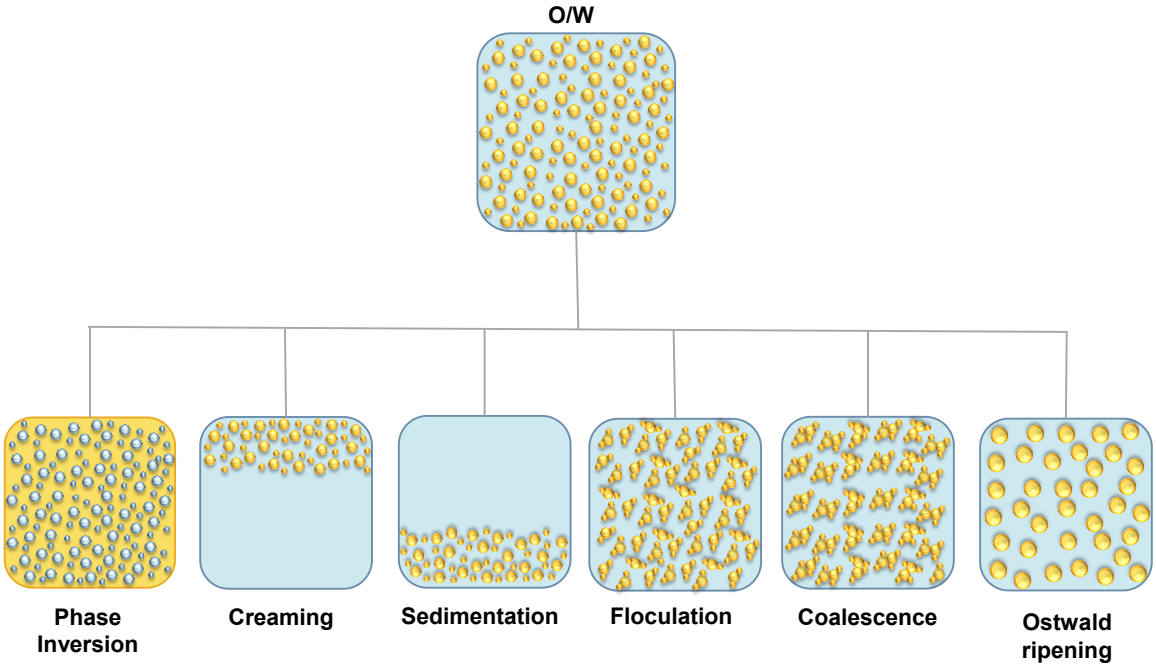

Figure 7 - Representation of physical instabilities in emulsions.
Source: adapted from Barranco, L. M. D.; Castro, R. M. L. [20,23].

Emulsifiers are used to avoid instabilities. Surfactants, also called emulsifiers, consist of organic molecules with a hydrophobic (apolar) and hydrophilic (polar) region, called amphoteric or amphiphilic molecules, as shown in Figure 8. Thus, they present double affinity behavior, interacting with the aqueous phase through its polar part and with the oily phase through its apolar region (Figure 8) [17,21].

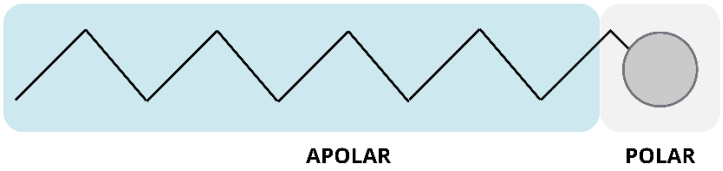

Figure 8 - Representation of the surfactant molecule.
Source: adapted from Ferreira P. G. *et al* [17].

The role of an emulsifier is to reduce the surface tension and create an electrostatic repulsion between the phases, acting against the coalescence of the droplets, forming a stable system due to its action as a stabilizing agent of the emulsion [7,20,23]. Surfactants can be classified according to Table 1. Generally, the most used surfactants are ionic (anionic and cationic) due to advantages over others, such as low cost, greater stability, low sensitivity, and low toxicity [20,25].

Table 1 - Classification of surfactants.

TYPE	MECHANISM	APPLICATIONS	REPRESENTATION
Anionic	Presents negative charge in the hydrophilic region	Soaps, sulfated and sulfonated compounds	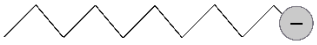
Cationic	Has a positive charge in the hydrophilic part	Conditioners, creams, and oil extraction	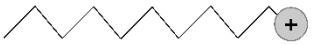
Non-ionic	Characterized by having non-charged hydrophilic groups in its structure	Detergents, emulsifying agents, wetting agents, solubilisers, and degreasers	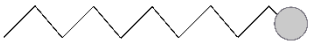
Amphoteric	In the hydrophilic part it has both positive and negative charges and its main characteristic is the change of charge as a function of pH	Drugs realese and lecithins	

Source: adapted from Caldeira, G. *et al*; Castro, R. M. L.; Ferreira, P. G. *et al* [17,20,25].

However, the excessive use of synthetic surfactants in emulsions has disadvantages such as water pollution and non-degradability and, in cosmetic products, can cause adverse effects such as allergies, inflammation, and dermatitis [5–7,24,26,27]. Thus, Pickering emulsions, formed without molecular surfactants, are gaining ground as a safe, sustainable, and ecologically friendly alternative to conventional emulsions.

2.5. Pickering emulsions

Pickering emulsions were discovered in 1903 by Ramsden when his studies revealed that solid particles adsorbed and stabilized air-water interfaces [7,27]. Later, in 1907, Pickering's studies showed that solid particles stabilized O/W emulsions. Pickering compared conventional emulsions with emulsions stabilized by solid particles and concluded that the latter had greater stability. In addition, it was described how the stability of the emulsions was related to the size and wettability of the solid particles, both in the aqueous and in the oily phase [24,26–28].

Pickering emulsions are stabilized by particles rather than molecular surfactants, like in conventional emulsions, as show in Figure 9 [7,24,29]. The solid particles allow the balance

between the oily phase and aqueous phase by being absorbed onto the oil surface, developing a greater stability of these emulsions and thus giving a high resistance to coalescence [24].

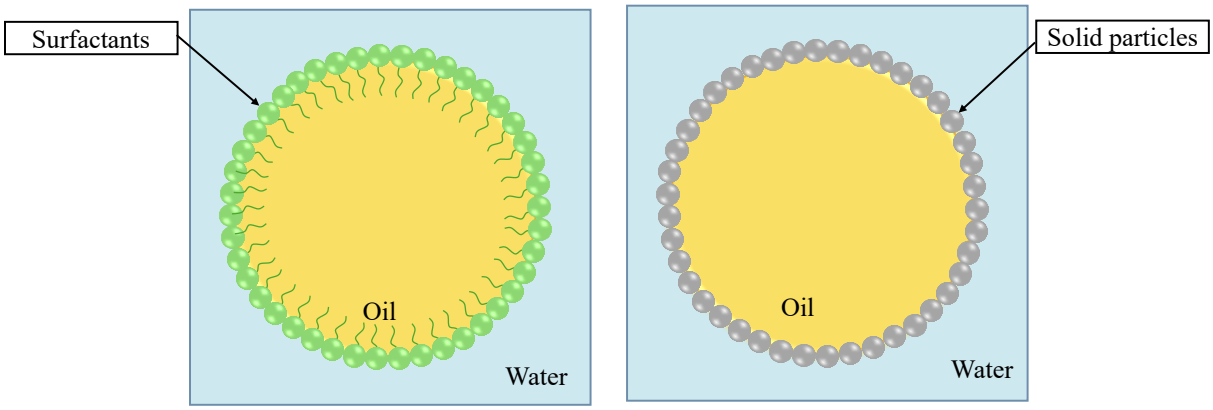

Figure 9 - Illustration of a conventional emulsion (based on surfactant) and Pickering emulsion. Source: adapted from Chevalier, Y.; Bolzinger, M. [26].

Unlike conventional emulsifiers, solid particles do not generate a decrease in interfacial tension between the oily and aqueous phases. Due to high adsorption energy, they stabilize the emulsion by forming a physical barrier between the droplets of the dispersed phase and the continuous phase. In this way, the particles are irreversibly adsorbed at the two-phase interface, making the coalescence take longer to occur. In addition, the particles interact with each other to form a three-dimensional structure in the continuous phase, increasing the viscosity and decreasing the speed of migration of the droplets [7,23].

For solid particles to act as stabilizers, they need to be partially wettable by both phases and have adequate size and concentration [6,7,23]. Thus, the particle position in the interfacial plane, i.e., the particle wettability, is essential to predict the emulsion stabilization and the type preferentially formed [6,23].

The emulsion type (O/W or W/O) is defined by the wettability of the particle positioned at the oil-water interface, and its relative affinity in both phases is characterized by the three-phase contact angle (θ) [28]. Thus, particles having $\theta < 90^{o}$ tend to form O/W emulsions, due to their more hydrophilic character, while particles with $\theta > 90^{o}$ tend to form W/O emulsions due to their more hydrophobic character, as show in Figure 10 and Figure 11 [23,28]. The particles with θ equal or very close to 90^{o} are considered amphiphilic particles for presenting affinity with both phases [23,30]. In contrast, at θ values outside these ranges, the particles are either too hydrophilic (close to 0◦) or too hydrophobic (close to 180◦) to be adsorbed at the oil-water interface [27].

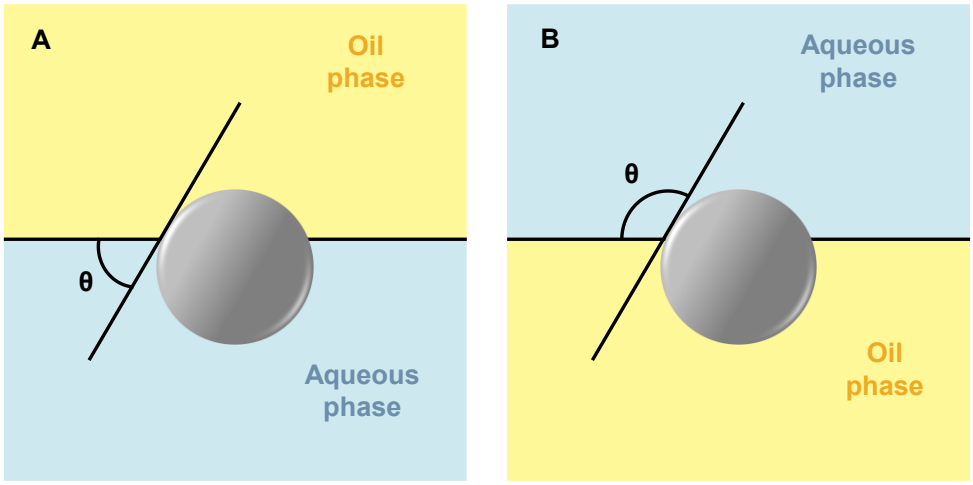

Figure 10 - Wettability mechanism in W/O and O/W Pickering emulsions: (A) the particle at the emulsion interface with θ < 90° and (B) the particle at the emulsion interface with θ > 90°.
Source: adapted from Peito, S. G. P. [20].

In addition, the relative affinity of the particles for the oily phase and the aqueous phase is defined by Young's equation, Equation (1), where $\gamma_{po}, \gamma_{pw}, \gamma_{ow}$ are, respectively, the particle-oil, particle-water and oil-water interfacial tensions [31].

$$\cos\theta = \frac{\gamma_{po} - \gamma_{pw}}{\gamma_{ow}} \quad (1)$$

The properties of the oil phase, such as its polarity and viscosity, directly influence the contact angle between the phases, which can compromise stabilization efficiency, as well as having an impact on the diameter of the droplets and even the type of emulsion formed. Another determining factor is the ratio between the system's phases, since an increase in the dispersed fraction tends to generate larger droplets. In this scenario, a constant quantity of stabilizing particles may not be enough to cover the entire interface generated, reducing the stability of the emulsion [32].

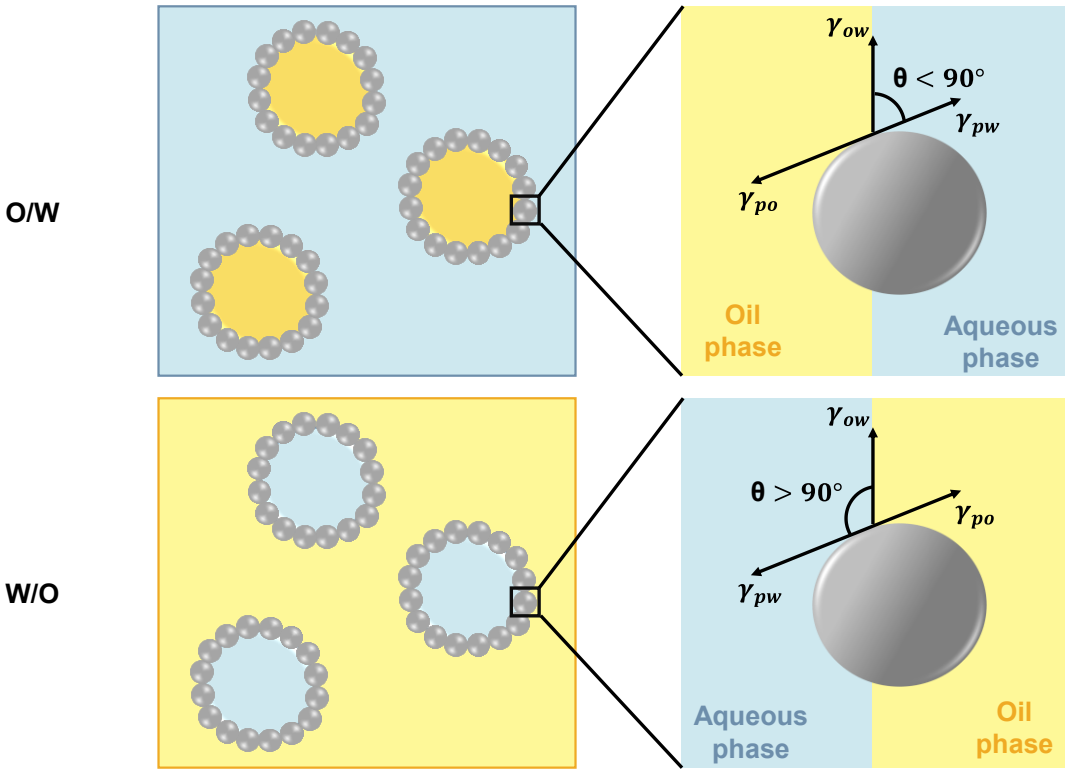

Figure 11 - Representation of O/W and W/O Pickering emulsion systems and the geometrical definition of the three-phase contact angle (θ) as a function of the particle–oil (γpo), particle–water (γpw), and oil-water (γow) interfacial tensions.
Source: adapted from Guzmán, E.; Ortega, F.; Rubio, R. G. [6].

Pickering emulsions are relevant systems for designing surfactant-free cosmetic products. In the pharmaceutical field, where the delivery of transdermal and dermal drugs is difficult to achieve and the release of medications is desired, they are becoming essential systems [32]. Furthermore, the surfactant-free nature of Pickering emulsions also confers to them a more sustainable and eco-friendly character compared to conventional emulsions[5,7].

Currently, Pickering emulsions have wide applications in the pharmaceutical, biomedical, food, material engineering, crude oil recovery, catalysis, cosmetics, among others [24,33]. In the cosmetic industry, Pickering emulsions are powerful systems reported to increase the depth of active penetration into the skin, allowing the preparation of skincare products with sensory pleasant to the touch, low irritability, and high product stability [7].

2.6. Application of Pickering emulsions in the cosmetic industry

Sustainable cosmetics are gaining increasing interest in industrial sectors due to consumer demands for safer and more sustainable products. Cosmetic emulsions, such as lotions, gels, and creams, contain surfactants to disperse and emulsify the oily phase. Even

though surfactants are very popular in cosmetics, some studies show that they have adverse effects on the environment and human health and can cause adverse skin reactions such as inflammation and contact dermatitis [5].

As a sustainable alternative to surfactants, Pickering emulsions have been gaining attention in cosmetic applications where conventional surfactants are replaced by solid particles to eliminate or significantly reduce toxicity and irritation from using synthetic surfactants [5]. At the same time, using solid nanoparticles can improve emulsion droplet stiffness, resulting in a controlled release, high incorporation, and transdermal adsorption of assets [6].

However, studies of Pickering emulsions development for cosmetic applications are limited due to the restriction of cosmetically acceptable compounds [6]. Wu *et al.*[34] developed a study of the preparation of Pickering emulsions stabilized with silica nanoparticles using different cosmetically acceptable oils in cosmetology, such as silicone and ester oils. Such studies have shown that solid particles of distinct nature are necessary to prepare emulsions depending on oil nature. Terescenco *et al*. [35] conducted a study comparing the textures of Pickering emulsions stabilized with three types of solid particles (TiO_2, SiO_2, and ZnO) with conventional emulsions stabilized by surfactants. The study found that emulsions stabilized by solid particles showed a texture more opaque and less greasy than emulsions stabilized by surfactant. Thus, it was demonstrated that Pickering emulsions present better sensory attributes than conventional emulsions, which are preferable for cosmetic applications due to absorption, spreadability, and stability [6].

The contributions of Pickering emulsions for cosmetic applications can improve the stability of cosmetic formulations to external environmental stresses such as heating, pH, or irradiation, increase the shelf life of cosmetic formulations, and exert a controlled release of the active principle. In addition, a case-by-case study of the toxicity of Pickering emulsions and their biological effects on skin sensitivity and irritation is necessary. An alternative to minimize the potential adverse effects is using bio-based particles as stabilizers [6].

2.7. Pickering stabilizers

Nanoparticles, colloidal particles, or microparticles can substitute synthetic surfactants and stabilize Pickering emulsions [25]. Some important parameters for determining the effectiveness of particles in stabilizing the emulsion are shape, size, concentration, particle wettability, and interactions between them [27,31].

The emulsion droplet size is directly related to particle concentration. The phenomenon called "limited coalescence" shows that, for a fix O/W ratio, the droplet size decreases when the particle concentration increases; thus, it is possible to obtain emulsions with controlled droplet size. The emulsions present a homogeneous droplet size distribution, directly proportional to the used particles amount and the coverage of the droplets, described by Equation (2) [24,31]. In Equation (2), D represents the final diameter of the emulsion droplet, m_p is the mass of the particles, ρ_p is the density of the particles, V_d is the volume of the dispersed phase, C is the surface coverage (fraction of the interfacial area of the drop that is covered by the particles), a_p the particle area projected on the interface, and ϑ_p is the volume of the particle [31].

$$\frac{1}{D} = \frac{m_p}{6\ x\ C\ x\ \rho_p\ x\ V_d} \frac{a_p}{\vartheta_p} \qquad (2)$$

The shape of the particles determines their behavior at the interface. Particles may take the form of fibrils, spheres, globules, or platelets and serve as a physical barrier in Pickering emulsions (Figure 12) [31,36].

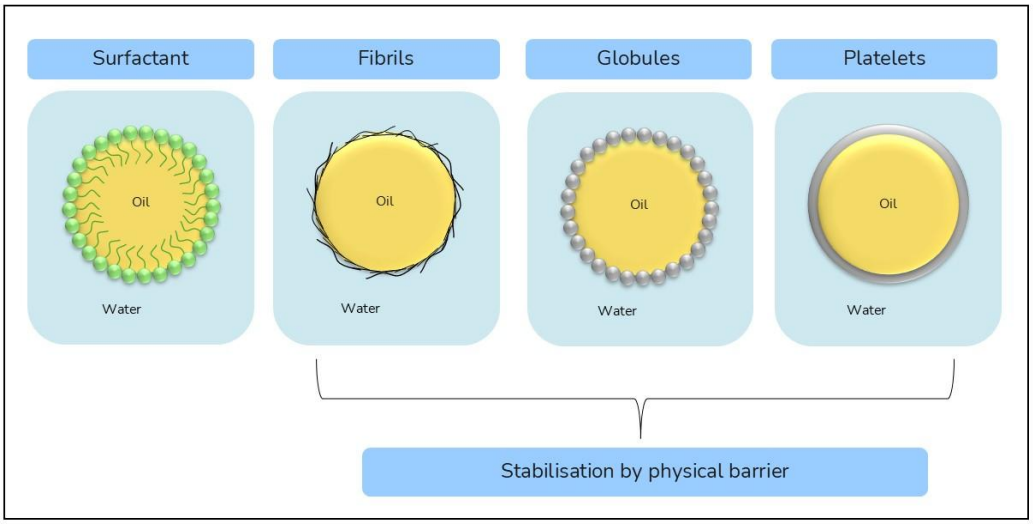

Figure 12 - Representation of oil droplet stabilization using molecular surfactant and different type of particles. Source: adapted from Calabrese, V. *et al* [36].

The particle concentration significantly influences the stability and droplet size of Pickering emulsions. At low particle concentrations, only a limited interfacial area can be

stabilized, resulting in larger droplet sizes and reduced emulsion stability. At intermediate particle concentrations, the available particles are insufficient to fully cover the increased interfacial area, leading to droplet coalescence until the surface is adequately covered. In contrast, high particle concentrations may allow an excess of particles to remain suspended in the continuous phase, promoting the formation of stable and often more viscous emulsions[31].

A wide range of organic and inorganic particles can be applied as Pickering stabilizers (Table 2). Inorganic materials include silica particles, which are widely used in the formulation of W/O Pickering emulsions, with silicone oil as the oil phase, aimed at the controlled release of drugs and topical applications [32,37]. Another example of an inorganic particle is montmorillonite (MMT), a type of natural clay used to stabilize Pickering O/A emulsions using liquid paraffin as the disperse phase [38]. Organic particles include cellulose particles used to stabilize Pickering O/A emulsions with hexadecane as the oil phase [39], as well as lignin particles used in formulations with Mygliol 812 oil for cosmetic applications[33,40].

Table 2 - Classification of solid particles.

TYPE	EXAMPLES	REFERENCES
Organics	Proteins, Polysaccharides, Lipids, Chitosan, Cellulose nanocrystals	[24,33]
Inorganics	Metals, Calcium carbonate, Barium sulphate, Clays, Silicas	[26,33]

2.8. Humic acid

Humic substances (HSs) are the most abundant biopolymers in the world. Living organisms synthesized them through humification for millions of years [8]. Humic substances are classified according to their solubility in aqueous solutions and are divided into humic acid, fulvic acid, and humin [41]. Humic acid (HA) corresponds to the fraction that is soluble in alkaline solutions, while fulvic acid is the fraction that is soluble in water, regardless of pH. Humin, conversely, represents the fraction that remains insoluble in any pH range [42,43].

HAs belong to a group of polymers with high molecular weight macromolecules. They are found in soils, waters, and sediments, resulting from the decomposition of plants and natural waste. They can also be obtained through secondary processes, such as the polymerization of polyphenols leached by rain and the condensation of phenols, quinones, and proteins by soil microorganisms [44,45].

Commercial HAs are traditionally extracted from non-renewable carbon sources such as peat and coal. However, recent studies, such as Azevedo's [46], show that these compounds can also be obtained from natural matrices such as water, soil, and sediment. Alternatively, more sustainable methods have been explored, including fermentation using plant waste such as palm fruit agglomerates, a renewable and ecologically viable source. In addition to natural and biotechnological routes, HA can be synthesized through chemical reactions, such as the polymerization or condensation of organic precursors [8,44].

The composition of the HAs varies according to the source origin, age, climate, and environmental conditions of extraction and production. Phenolic, carboxylic, enylic, quinone, and ether functional groups are present in their chemical structure, as shown in Figure 13, but may also include sugars and peptides [8,44]. The large structure of a HA molecule is composed of hydrophilic parts, consisting of OH groups, and hydrophobic parts, consisting of aliphatic chains and aromatic rings [44].

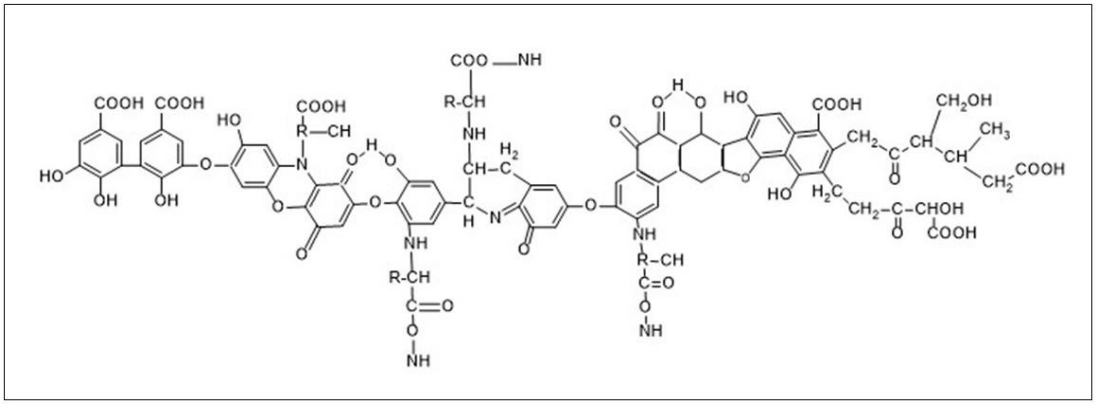

Figure 13 - Representative scheme of the structure of humic acid.
Source: adapted from Melo, B. A. G.; Motta, F. L.; Santana, M. H. A. [44].

Due to its antiviral, antimicrobial, antibacterial, and anti-inflammatory activities, HA can be applied in several areas, such as pharmaceutical, medicine, veterinary, and, more recently, cosmetic/dermo-cosmetics [8,47]. According to Figure 14, HA can be found on the market for different purposes, such as fertilizer in agriculture, food supplements, and cosmetics [8,47].

Figure 14 - Products containing humic acid. (A) Fertilizer Codahumus 20 from the company Hubel Verde, (B) Food supplement Nutricology, (C) Rocky Mountain shower gel, and (D) Treatment ampoules for skin brand Trawenmoor.

In the cosmetic field, HA has been shown to promote collagen production, inhibit free radicals, stimulate tissue repair, reduce inflammation in cases of burns, and provide significant protection against UV-B radiation [8]. Therefore, HA has a high potential for cosmetic application, given that consumers seek products with these benefits, especially those related to skincare, a growing sector with a high representation in the cosmetic industry.

2.9. Acid precipitation method for particle synthesis

The acid precipitation method is widely used to produce particles and nanoparticles, especially in colloidal systems. This technique is based on the solubilization of a polymer in an alkaline medium, followed by particle precipitation by adding a non-solvent, in this case, an acid. The mechanism of acid precipitation involves the reduction of solute solubility through controlled acidification, resulting in the formation of small-sized particles [47,48].

HA is soluble in alkaline media and, due to its long polymeric chain with both hydrophobic and hydrophilic segments, it adopts an extended configuration due to the deprotonation of carboxylic and hydroxyl groups and the repulsion between negative charges. However, upon adding an acid, the cations in the medium reduce this electrostatic repulsion, allowing the polymer chain to fold into a more compact structure. In this state, the hydrophobic regions of the HA remain in the core, while the hydrophilic portions are exposed toward the surface, facilitating its precipitation [48].

3. Methodology

3.1. Materials

HA was purchased from Sigma Aldrich. A 0.5 mol/L sodium hydroxide solution was prepared using sodium hydroxide from Panreac with 99% purity. A 0.5 mol/L acetic acid solution was prepared using acetic acid (Honeywell Fluka), and a 0.5 mol/L citric acid solution was prepared using citric acid (Merck). Olive oil was obtained from Fagron (Spain), Miglyol 812 from Acofarma (Spain), and sweet almond oil from LabChem (Portugal). The used water was distilled water.

3.2. Screening of HA solubility

The solubility of HA was evaluated in different solvents (deionized water, ethanol, acetone, HCl solution, and NaOH solution) at various pH values (pH 2, 4, 6, 8, 10, and 12). A concentration of 30 g/L of HA was used for the study, and the sample was dissolved in the selected solvent using an ultrasound bath for 30 minutes. After solubilization, the mixture was centrifuged to separate the phases. The supernatant was removed, and the insoluble phase was dried in an oven. The mass of soluble fraction (m_3) was calculated based on the difference between the initial mass of HA (m_1) and the final mass of the dried insoluble fraction (m_2). The percentage of the soluble fraction (% Sol) was determined by the ratio between m_3 and m_1, as described in Equation (3).

$$\% \, Sol = \frac{m_1 - m_2}{m_1} * 100 = \frac{m_3}{m_1} * 100 \quad (3)$$

3.3. Screening of HA Pickering potential using different oils

Pickering emulsions were prepared using raw HA at a concentration of 30 g/L with different oils, such as Mygliol 812, sweet almond oil, and olive oil, in order to evaluate the Pickering potential of HA particles using different oils.

The O/W Pickering emulsions were produced following previously established protocols developed by the group [49]. For this purpose, the raw HA was initially dispersed in a 0.5 M sodium hydroxide solution, from which 10 mL were collected for the preparation of the emulsions. The aqueous phase containing the HA was homogenized using a rotor-stator homogenizer (CAT Unidrive X 1000, Germany) for 2 minutes at 13,500 rpm. Subsequently, 10 mL of the oil phase were slowly added to the aqueous phase using a peristaltic pump at 1

mL/min (Ismatec™ MS-CA Series, Thermo Fisher Scientific, USA) and further dispersed using the rotor-stator homogenizer operating at 13,500 rpm for 5 minutes, as shown in Figure 15.

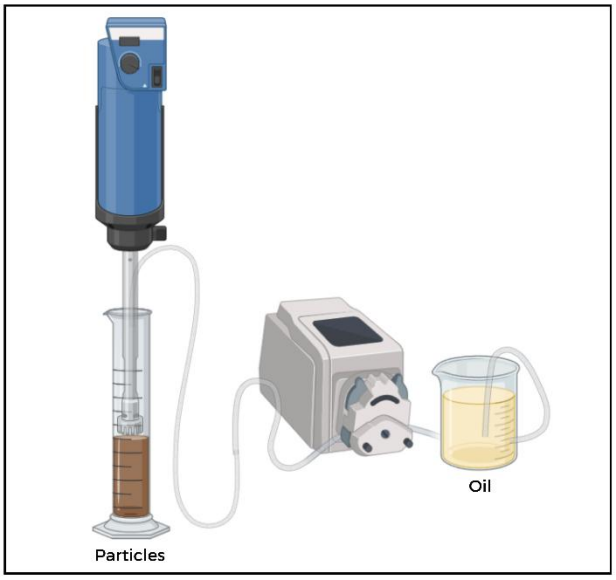

Figure 15 - Diagram of Pickering emulsion production.

3.4 Production of HA particles through acid precipitation

HA particles were obtained by acid precipitation, based on the methodology described by Steven Cowling [50], with some modifications. Initially, HA was dissolved in 0.5 M NaOH solution at 30 g/L. The mixture was kept under stirring for 24 hours at room temperature. After this period, the sample was centrifuged (Centrifuge 5810 R, Eppendorf, Germany) at 10,000 rpm for 20 min to separate the insoluble and soluble fractions. The HA soluble fraction was collected, and the insoluble fraction was dried to quantify both fractions. Before preparing the particles, the HA concentration in the soluble fraction was adjusted to the desired value with 0.5 M NaOH solution. After this, HA particles were produced by adjusting the pH of the HA soluble fraction with acetic or citric acids to values of 5, 7, and 9, as shown in Figure 16.

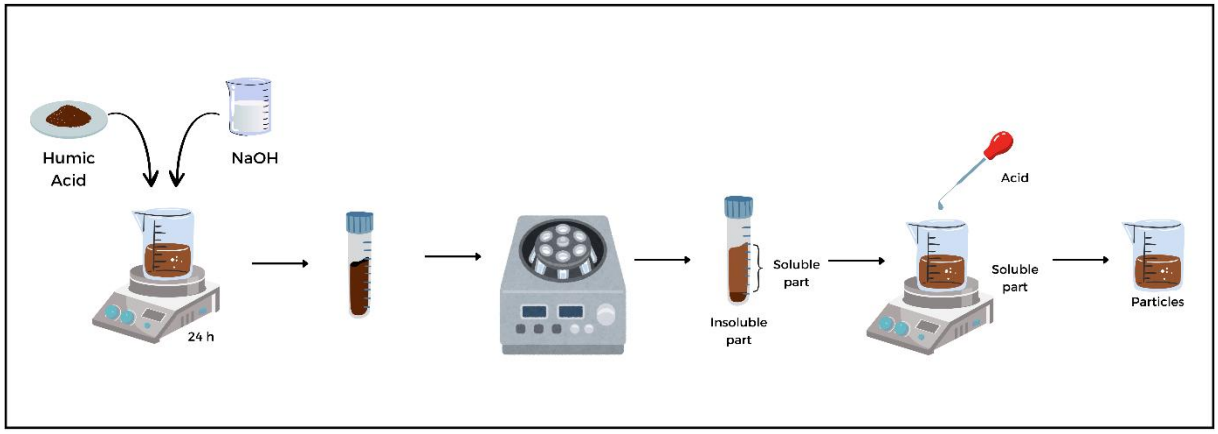

Figure 16 - Diagram of the production of humic acid particles by the acid precipitation method.

3.5 Preparation of O/W Pickering emulsions

The O/W Pickering emulsions were prepared according to protocols previously developed by the research group [49], with minor modifications. The particles obtained via acid precipitation were combined with sweet almond oil at different oil volume percentages (50%, 55%, 60%, 65%, 70%). Initially, the aqueous phase containing the HA particles was dispersed using a rotor-stator homogenizer (CAT Unidrive X 1000, Germany) for 2 minutes at 13,500 rpm. Then, the oil phase was slowly added to the aqueous phase using a peristaltic pump (Ismatec™ MS-CA Series, Thermo Fisher Scientific, USA) at 1mL/min and further dispersed using the rotor-stator homogenizer, operating at 13,500 rpm for 5 minutes to form the emulsion.

3.6 Characterization

3.6.1 Particle size and zeta potential

The particle size and zeta potential were determined by dynamic light scattering (DLS) using a Zetasizer Ultra instrument (Malvern Panalytical Ltd., United Kingdom). For the analyses, the particles were diluted with distilled water at a 1:100 (v/v) ratio and placed in a standard DTS1070 disposable folded capillary cell. All measurements were performed in triplicate at room temperature, and the results are presented as mean ± standard deviation.

3.6.2 Morphology

The morphology of the particles and emulsions was evaluated by optical microscopy using a Nikon Eclipse 50i microscope (Nikon Corporation, Japan) equipped with a Nikon Digital system at different magnifications (100x, 200x, and 400x) [51]. An aliquot of the sample was placed on a microscope slide and covered with a coverslip. Image acquisition and processing were performed using the NIS-Elements Documentation software.

Transmission electron microscopy (TEM) was used to analyze the morphology of the particles. For this, the particles were diluted with distilled water at a 1:200 (v/v) ratio; then 10 μL of the sample was placed on nickel grids coated with a carbon/Formvar film (Electron Microscopy Sciences, Hatfield, PA, USA), allowed to rest for 2 minutes. The excess liquid was removed with filter paper. Visualization was done using a JEOL JEM 1400 TEM at 120 kV (Tokyo, Japan), and images were acquired with an Orius 1100 W CCD digital camera (Tokyo, Japan).

The interfacial microstructure of the emulsion was analyzed by confocal microscopy (Leica TCS-SP5 AOBS, Leica Microsystems Inc. Heidelberg, Germany). The emulsion was placed on concave slides, and the HA autofluorescence was inspected using an argon laser (excitation at 488 nm and emission at 503-598 nm). Additionally, the emulsion was stained with the fluorescent dye Nile Red in isopropanol (0.1% w/v) and analyzed using a UV laser (excitation at 405 nm and emission at 503-598 nm). Images were acquired using a 40x/1.3 magnification lens.

3.6.3 Three-phase contact angle

The three-phase contact angle, formed between the particle surface, oil, and aqueous phase, was determined using a goniometer (model 210, Ramé-hart Instrument Co., USA), according to the methodology described by Colucci *et al* [51]. For the analysis, the particles were previously dried at 40 °C for 72 hours and then compressed into pellets with a diameter of 13 mm and a thickness of 2 mm using a hydraulic press (Specac Ltd., United Kingdom) at a pressure of 9 tons for 1 minute and 30 seconds. The contact angle was measured at room temperature using the sessile drop method by depositing a 5 μL drop of water onto the pellet's surface [51]. The drop was monitored for 30 seconds using a camera attached to the goniometer, and contact angles were measured in triplicate. The results are presented as the average values recorded during the monitoring period.

3.6.4 Dialysis

The yield of HA particles after acid precipitation was performed through dialysis. The particle dispersion (70 mL) was placed in a dialysis bag (Spectrum™ Labs Spectra/Por™ 1, 6–8 kDa MWCO Standard RC Dry Dialysis) and immersed in a beaker containing water (2 L). The external water phase was replaced every 3 to 4 hours until stabilization of electrical conductivity was achieved, indicating the removal of salts and other soluble impurities. The

yield of HA particles was calculated based on the ratio between the initial mass of soluble HA (m_1) and the final mass after dialysis (m_2), as described in Equation (4).

$$Yield\ (\%) = \frac{m_1}{m_2} * 100 \quad (4)$$

3.6.5 Emulsion droplet size

The droplet size of the emulsions was determined by laser diffraction using a Mastersizer 3000 instrument, coupled with a Hydro MV dispersion unit (Malvern Instruments Ltd., United Kingdom). Samples were added to the dispersion medium (water) until reaching an obscuration level of approximately 7%, under a stirring speed of 2000 rpm at room temperature. Measurements were performed in five consecutive readings per sample, and the results were expressed as a volume-based size distribution. Emulsion droplet size was represented by the volume-weighted mean diameter D[4,3], also known as De Brouckere mean diameter.

3.6.6 Emulsion stability

The stability of the emulsion was evaluated through macroscopic and microscopic parameters, namely by the percentage of emulsified layer formed (% EL) and the emulsion instability index (EII), respectively.

The ability of the emulsified system to form and maintain a stable continuous phase was quantified using the percentage of emulsified layer (% EL), calculated based on the ratio between the height of the emulsion layer (He) and the total height of the sample (Ht), according to Equation (5) [51].

$$\%\ EL = \frac{He}{Ht} * 100 \quad (5)$$

The samples were evaluated after 1, 7, 15, and 30 or 45 of production.

Microscopic stability was assessed using the emulsion instability index (EII), determined according to Equation (6) [52].

$$EII = \frac{d(t) - d(0)}{d(0) * t} \quad (6)$$

Where d(0) represents the average droplet diameter at the initial time and d(t) is the average droplet diameter after a given time t. In this work, d(0) and d(t) corresponded to the emulsion average droplet size, D[4,3], after 1 and 30 days of storage, respectively. The EII values were interpreted according to the following criteria:

- 0< EII < 0.05: Highly stable
- 0.05 < EII < 0.5: Moderately stable
- 0.5 < EII < 5.0: Moderately unstable
- EII > 5.0: Highly unstable

3.6.7 Antioxidant activity

The antioxidant activity of the emulsions was determined using the 2,2-diphenyl-1-picrylhydrazyl (DPPH) radical method, according to Brand-Williams [53], with minor modifications. For this purpose, the samples were diluted to various concentrations (ranging from 0.005 to 2000 μg/mL) using DMSO as the solvent. Subsequently, 30 μL of each dilution were transferred to a 96-well microplate and mixed with 270 μL of a methanolic DPPH solution (6 x 10^{-5} mol/L). The mixture was incubated for 30 minutes in the dark at room temperature. The reduction of the DPPH radical was monitored by spectrophotometry, measuring absorbance at 517 nm using a microplate reader (Epoch, Agilent, USA). Antioxidant activity was calculated based on the inhibition percentage of DPPH radical, according to Equation (7), where Ac corresponds to the absorbance of the DPPH solution without sample (control), and As to the absorbance of the DPPH solution with the tested sample.

$$\%\ Inhibition = \frac{(A_C - A_s)}{A_C} * 100 \quad (7)$$

3.6.8 Rheological analysis

The viscous and viscoelastic behavior of the emulsion was analyzed using a parallel plate with serrated surface (20 mm) geometry in the rheometer (Kinexus Prime lab+, NETZSCH, Germany) with a gap size of 0.6 mm at 25 ºC. The dynamic viscosity was determined as a function of the shear rate from 0.1 to 1000 1/s. The frequency sweep oscillated from 0.1 to 10 Hz, and all measurements were performed within the determined linear

viscoelastic region (LVE) at a 0.1 % shear strain. Data was reported as storage modulus (G') and loss modulus (G") as a function of frequency [40].

3.6.9 Texture analysis

The optimized emulsion's texture was characterized according to the methodology described by Oliveira [54], using the Stable Micro Systems texture analyzer equipped with the "Backward Extrusion Rig" accessory. This accessory consists of an extrusion disk with a diameter of 35 mm, and a 5 kg load cell was used.

The disc was positioned centrally in the sample container for the tests, with a standardized height of 45 mm of product. The test began with the disk at 40 mm above the sample's surface, and was then inserted to a depth of 20 mm, at a constant speed of 1 mm/s. After each analysis, the probe was returned to the starting position (40 mm above the sample), ensuring reproducibility and comparability of results between different formulations. The disc was carefully sanitized between tests to avoid cross-contamination between samples.

During the probe's recoil phase, the container was held steady by hand to avoid displacement caused by the product's resistance to the extraction movement.

The data was obtained using the Exponent software, which provided the following rheological parameters: maximum force, corresponding to firmness; positive area up to the peak, indicating consistency; maximum negative force, associated with cohesiveness; and area under the negative curve, which represents the "work of cohesion", reflecting the sample's resistance to removal from the disk and its viscosity.

In addition, the Spreadability Test was carried out on the same equipment, coupled to the Spreadability Rig (HDP/SR) accessory. For this test, the probe was positioned 25 mm from the sample's surface and inserted to a depth of 2 mm at a constant speed of 3 mm/s. After each measurement, the probe was returned to its initial position, and the accessory was sanitized between tests to ensure the integrity of the analyses.

The data was obtained using the Exponent software, which provided the following rheological parameters: maximum force, corresponding to the firmness of the sample; positive area up to the peak, indicating the shear force; maximum negative force associated with the stickiness property; and area under the negative curve, which represents the adhesion force of the sample.

3.6.10 Colorimetric analysis

The color of the emulsions was evaluated using a CR-400 colorimeter (Konica Minolta, Japan). The colorimetric parameters L*, a*, and b* (CIELAB space) were determined, where L* represents lightness, ranging from dark (0) to light (100). The a* value indicates the hue on the green-red axis, ranging from green (−60) to red (60), and b* expresses the hue on the blue-yellow axis, ranging from blue (−60) to yellow (60). [51]

4 Results and discussion

4.1 Humic acid solubility

HA is black in color, with heterogeneous particle size and irregular morphology. Its visual appearance and morphological characteristics are shown in Figure 17.

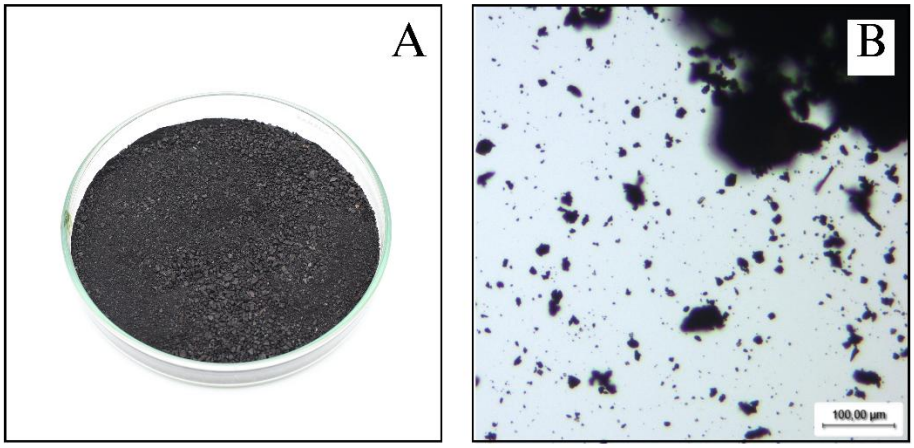

Figure 17 - (A) Photo of humic acid in natura and (B) optical microscopy of humic acid (100x magnification).

The solubility screening study of HA was carried out using a concentration of 30 g/L of HA in different solvents. The soluble fractions for each solvent are reported in Table 3.

Table 3 - Study of the solubility of humic acid at 30 g/L in different solvents.

Solvent	Humic acid soluble fraction (%)
Acetone	2.59 ± 0.15
Deionized Water	3.69 ± 0.05
Ethanol 60%	4.92 ± 2.92
Ethanol 70%	3.46 ± 0.07
Ethanol 80%	2.62 ± 0.02
Ethanol 90%	2.60 ± 0.32
Ethanol 100%	2.72 ± 0.40
HCl Solution (pH 2)	7.76 ± 0.90
HCl Solution (pH 4)	8.09 ± 0.08
HCl Solution (pH 6)	7.54 ± 0.40
NaOH Solution (pH 8)	8.02 ± 0.72
NaOH Solution (pH 10)	7.64 ± 0.51
NaOH Solution (pH 12)	38.01 ± 2.81

The highest soluble fraction of HA was achieved using NaOH solution at pH 12, which was selected as the solvent for particle production. An acidic solution was chosen as the

precipitating agent for forming solid HA particles, as the method is based on the principle of acid precipitation. The solubility of HA is favored in alkaline solutions, such as 0.5 M NaOH, where dissociation of acidic functional groups occurs. However, when adding an acid, the pH decreases, and these functional groups become deprotonated, reducing solubility and promoting the precipitation of HA in the form of particles [50].

It is noteworthy that HA showed low solubility in all solvents tested. According to the literature, its composition comprises different fractions: HA, fulvic acid, and humin. As reported by Cowling [50], when a humic substance is mixed in a 0.5 M NaOH solution, the humic and fulvic acids dissolve, while a significant amount of insoluble material, corresponding to humins, remains in solution. This low solubility can be attributed to the compositional characteristics of humic substances.

4.2 Potential of HA in natura to emulsify different oils

To evaluate the emulsifying potential of raw HA, Pickering emulsions were prepared using three different oils: sweet almond oil, Miglyol 812, and olive oil. Figure 18 shows the visual appearance of the emulsions and their morphology observed through optical microscopy.

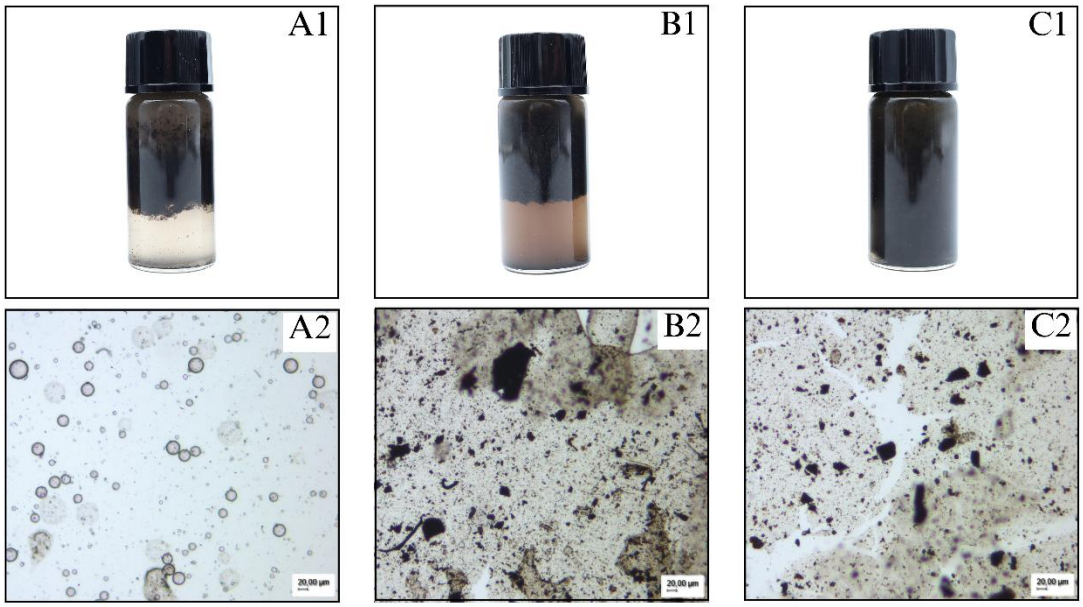

Figure 18 - Photo of Pickering emulsions (A1, B1 and C1) and corresponding optical microscopy (A2, B2 and C2) at 100× magnification. A1 and A2 emulsions with sweet almond oil; B1 and B2 emulsions with Mygliol 812 oil; C1 and C2 emulsions with olive oil.

The emulsion produced with sweet almond oil (Figure 18 A1) exhibited the best visual appearance, confirmed by optical microscopy analysis. The serum of this emulsion appeared clear, indicating a minimal amount of residual HA. In contrast, the optical microscopy images

of the emulsions prepared with Miglyol 812 (Figure 18 B1) and olive oil (Figure 18 C1) showed the presence of HA in large fragments, without the formation of droplets. This morphology resembles that observed in Figure 17 B, which shows the microscopy of raw HA, and differs from the homogeneous structure observed in the emulsion with sweet almond oil. Based on these results, sweet almond oil was selected as the oil phase for subsequent studies in emulsion production.

4.3 Effect of the pH in the production of humic acid particles through acid precipitation

Humic acid particles (HA-P) were produced from their soluble fraction in NaOH (pH 12) using the acid precipitation method with acetic acid and pH adjustment to values 5, 7, and 9. The morphology of the obtained particles is illustrated in Figure 19, while the size and zeta potential data are presented in Figure 20.

Figure 19 - Optical microscopy (50x magnification) of HA-P produced at (A): pH 5, (B): pH 7, and (C): pH 9.

In Figure 19 A, corresponding to HA-P precipitated at pH 5, a high quantity of particles with uniform morphology but greater aggregation is observed. This behavior can be explained by the fact that at acidic pH, HA solubility decreases, favoring particle formation and precipitation [48]. For HA-P precipitated at pH 7 (Figure 19 B), a considerable amount of particles is still present, though fewer than at pH 5. HA shows intermediate solubility at neutral pH, which may result in moderate precipitation. This suggests that the balance of electrostatic forces may favor the formation of smaller and more homogeneous particles [48]. In contrast, few HA-P are observed at pH 9 (Figure 19 C). This can be attributed to the higher solubility of HA in alkaline media, where it remains dissolved in solution rather than forming particles [50]. Therefore, the better particle formation conditions occurred at pH 5 and 7, which can be associated with the low solubility of HA at these pH levels.

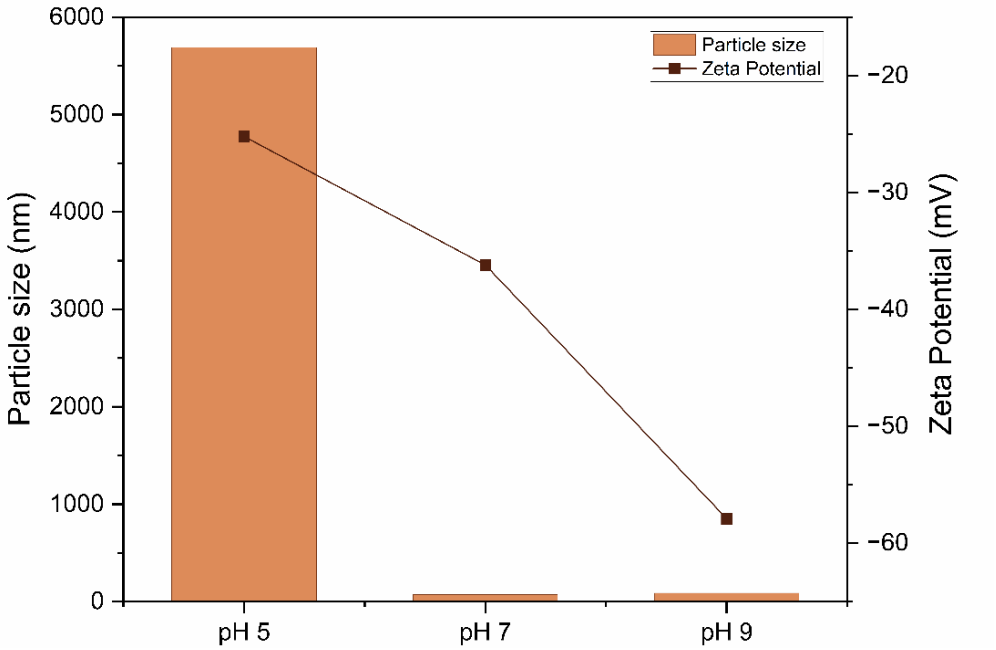

Figure 20 - Particle size and zeta potential of HA-P produced at pH 5, 7, and 9.

The particle size analysis showed that pH 5 HA-P were at least 65 times larger than those obtained at pH 7 and 9. In addition, as the pH increased, so did the zeta potential. This behavior is due to the dissociation of carboxylic and phenolic groups [55]. According to Prado [56], at low pH, the groups are protonated whereas at higher pH, a neutralization reaction occurs and the groups dissociate, becoming negatively charged. Thus, at pH 5, the groups are protonated and tend to carry neutral charges, causing particle aggregation and precipitation, which explains the larger size of these particles [55].

Zeta potential represents the charge balance on the surface of suspended particles and is a key parameter in predicting and controlling the stability of suspensions. High zeta potential values, whether positive or negative, indicate stronger electrostatic repulsion between particles, reducing aggregation tendencies and promoting system stability. This effect occurs because repulsion between charged droplets outweighs attractive forces, preventing coalescence and sedimentation [57]. Accordingly, HA-P at pH 5 exhibited lower zeta potential values than those at pH 7, indicating that the latter are more stable. In contrast, at pH 9, HA remained predominantly solubilized, meaning its molecules are dispersed in solution rather than forming solid particles, as corroborated by the optical microscopy in Figure 19 C. The high zeta potential indicates strong electrostatic repulsion between the few formed particles, preventing aggregation and promoting colloidal stability. The exact values for size and zeta potential are shown in Table A 1 in Appendix A.

The three-phase contact angle was measured using a pressed particle tablet, a water droplet, and a sweet almond oil medium. The pH 5 HA-P (Figure 21 A) and pH 7 HA-P (Figure 21 B) showed a hydrophilic character as perceived in Figure 19 where effective particle formation is shown. This process occurs through precipitation induced by an agent that reduces the solubility of HA in the medium, promoting a reorganization of its functional groups. During this reorganization, the hydrophobic groups tend to orient themselves towards the particles' core, while the hydrophilic groups position themselves on the surface. This configuration favors a more stable energy state in aqueous media. As a result, there is a reduction in the contact angle, indicating greater affinity with water. This behavior is characteristic of hydrophilic particles and facilitates their dispersion in aqueous systems [58,59]. On the other hand, at pH 9 (Figure 21 C), there was no obvious particle formation, as can be seen in Figure 19 C. In this alkaline condition, the humic acid remained dissolved as isolated macromolecules, due to the high ionization of the functional groups, which increases electrostatic repulsion and prevents aggregation. Thus, the contact angle observed reflected the presence of HA in the solubilized form. Figure 21 D shows the contact angle of HA in natura, revealing its strong hydrophobic nature and confirming the reorientation of the HA groups upon particle form[58,59].

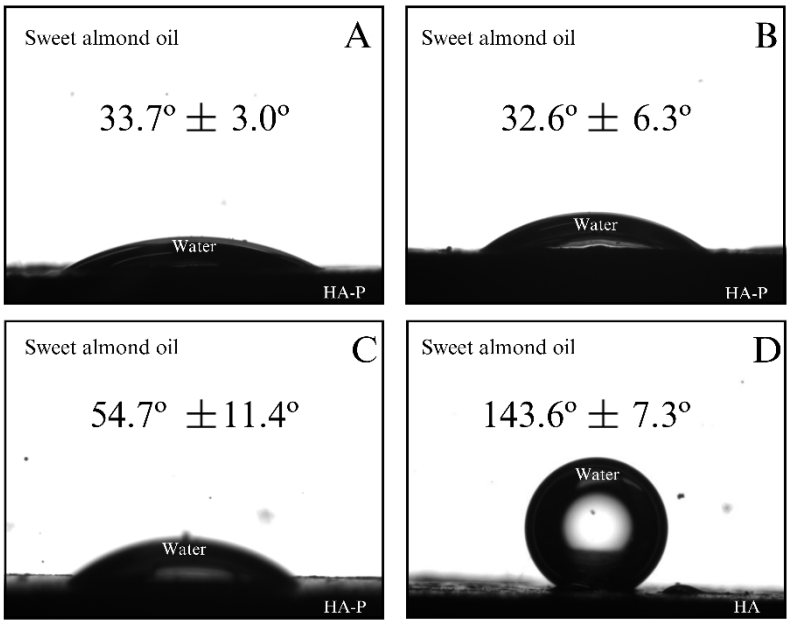

Figure 21 - Three-phase contact angle of HA-P produced at: (A) pH 5, (B) pH 7, and (C) pH 9 and (D) HA in natura.

Emulsions were then produced using the previously obtained particles, and Figure 22 shows their visual appearance and morphology as observed by optical microscopy.

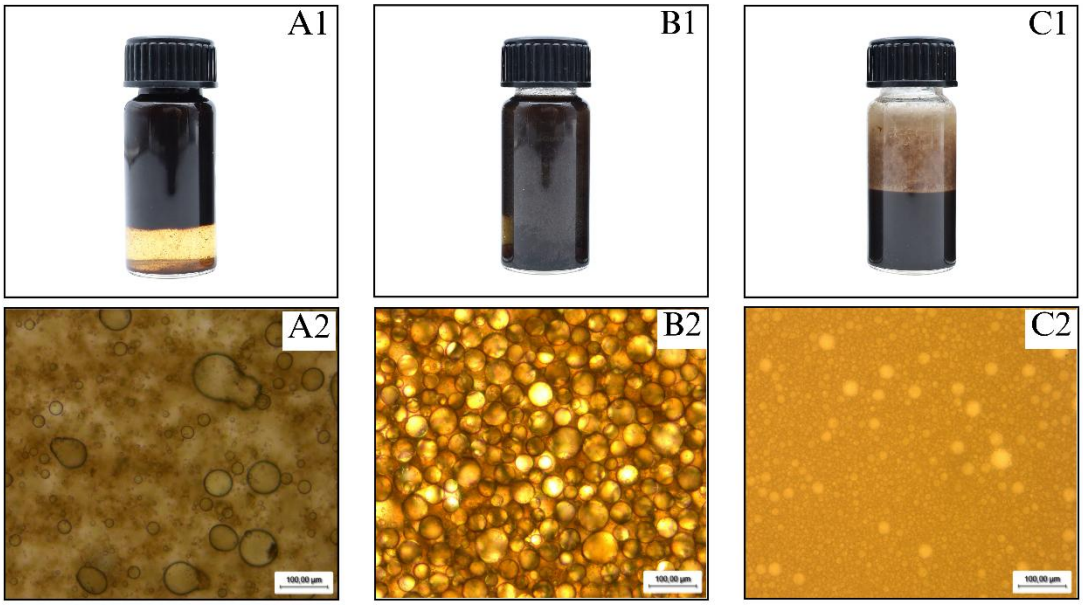

Figure 22 - Photo of Pickering emulsions (A1, B1 and C1) and corresponding optical microscopy (A2, B2 and C2) at 100x magnification. A1 and A2: emulsion with particles precipitated at pH 5; B1 and B2: emulsion with particles precipitated at pH 7; C1 and C2: emulsion with particles precipitated at pH 9.

The emulsion prepared with pH 5 HA-P exhibited a clearly defined serum layer, indicating that most HA-P was adsorbed in the emulsion structure. At the same time, the emulsified phase showed a dark brown color. On the other hand, the emulsion prepared with pH 7 HA-P presented a well-defined emulsified layer with a dark brown color and minimal serum. Moreover, the emulsion produced with pH 9 HA-P formed three distinct phases: a top layer of residual oil, a light brown emulsified layer, and a dark brown serum, indicating an excess of HA-P in this phase. Regarding morphology, the emulsion with pH 5 HA-P showed few small droplets with irregular shapes. In contrast, the emulsion prepared with pH 7 HA-P displayed highly concentrated, well-defined, rounded droplets. In contrast, the one stabilized with pH 9 HA-P exhibited smaller droplets. The best results were obtained with pH 7 HA-P since a higher emulsified layer was observed with a high concentration of well-defined spherical oil droplets. Thus, subsequent studies adopted the acid precipitation methodology with adjustments to pH 7.

4.4 Effect of the acid precipitating agent and HA concentration on particle formation and Pickering emulsion stabilization

A comparative study was conducted between two precipitating agents, acetic acid and citric acid, using different HA concentrations (4, 7, and 10 g/L – with the soluble fraction). To do this, the HA-P were produced using the same methodology described above, with a final

adjustment to pH 7. The morphology of the particles obtained is shown in Figure 23, while the data related to particle size and zeta potential are presented in Figure 24.

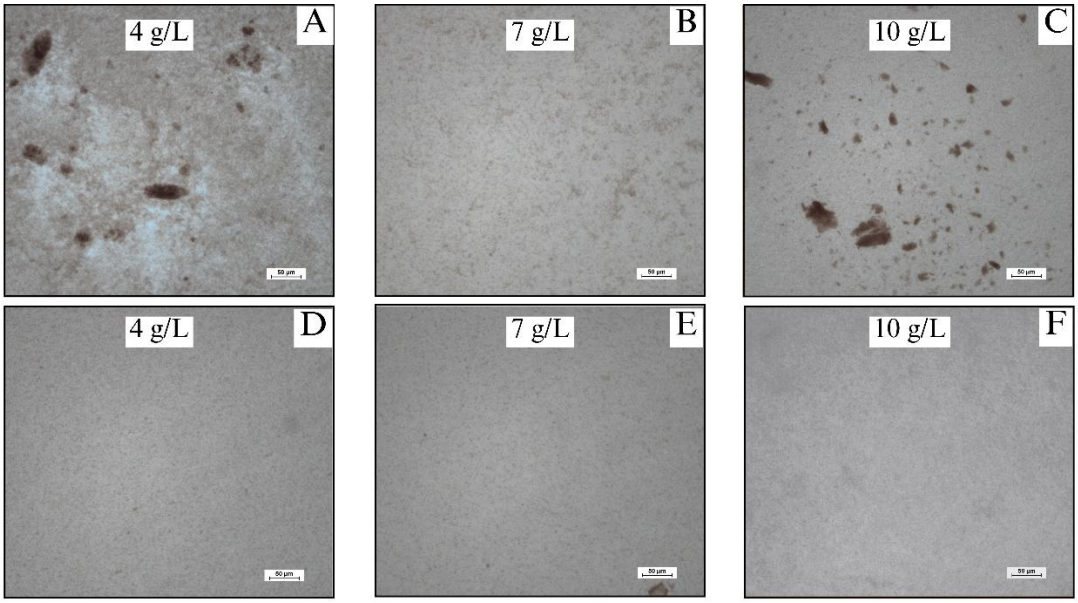

Figure 23 - Optical microscopy of the particles (100x magnification) produced with different concentrations of HA-P. A, B and C: particles precipitated with acetic acid and D, E and F: particles precipitated with citric acid.

Regarding the HA particles precipitated with acetic acid, it was observed that using a HA concentration of 4 g/L (Figure 23 A) resulted in the formation of larger and irregularly shaped particles. At a HA concentration of 7 g/L (Figure 23 B), particles were much smaller and more homogeneous, and the number of particles increased, showing a more uniform distribution. Particle agglomeration was observed at HA concentration of 10 g/L (Figure 23 C). In contrast, the particles precipitated with citric acid showed a different behavior than those with acetic acid. The particles were smaller and uniformly dispersed even at the lowest HA concentration (4 g/L, Figure 23 D). With increasing HA concentration to 7 and 10 g/L (Figure 23 E and F), the particles became more uniform and dispersed, with practically no visible agglomerates.

Figure 24 illustrates the obtained particle size and zeta potential of HA-P. Increasing the HA concentration reduced the particle size for both acetic and citric acid precipitating agents. At the same time, for acetic acid, the zeta potential decreased as concentration increased, showing that the particles were smaller and more stable at higher concentrations. For citric acid, the zeta potential started at more negative values at lower concentrations and remained similar at 7 and 10 g/L. Overall, the HA-P produced with citric acid was less influenced by variations in HA concentration, showing more consistent sizes ranging from 73.9 to 90.4 nm and a stable

negative zeta potential of approximately -40 mV. The obtained values for size and zeta potential are listed in Table A 2 in Appendix A.

According to Klucáková [60], the behavior of HAs is affected by two processes: the dissociation of acidic functional groups and the breakdown of humic aggregates into smaller molecules. Therefore, pH and concentration affect the spatial arrangement of these fractions. As concentration increases, particle size decreases, probably due to increased intermolecular interactions causing particles to spiral inward [60].

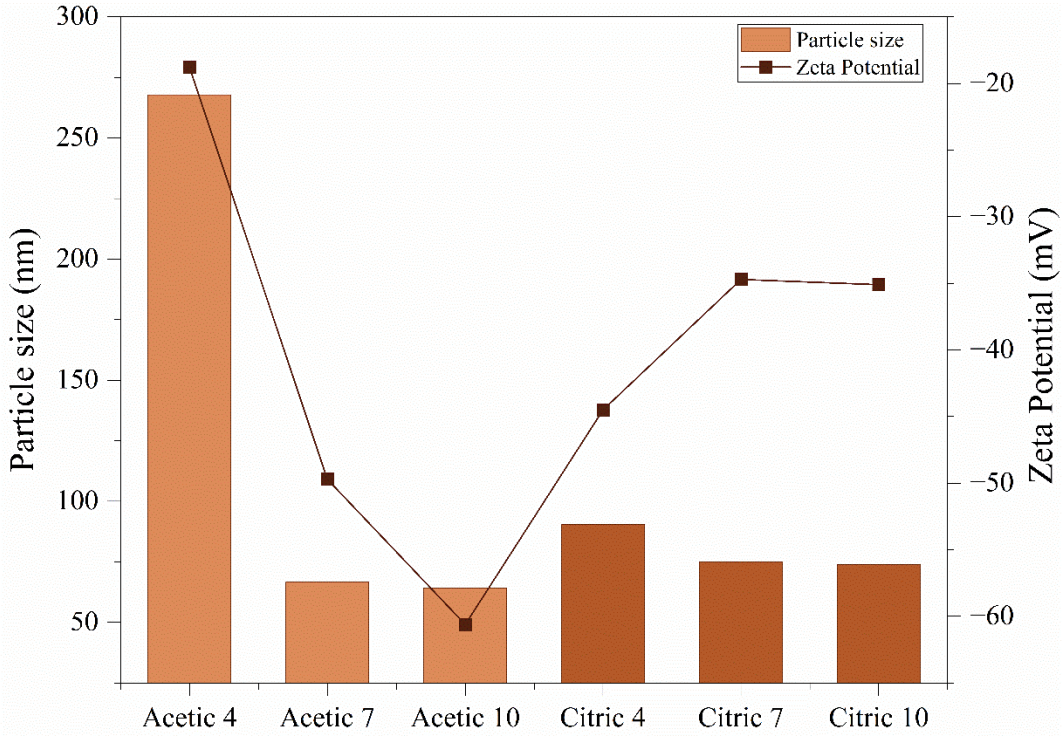

Figure 24 - Size and zeta potential of HA-P at concentrations of 4, 7, and 10 g/L using acetic or citric acid as precipitating agents.

Figure 25 shows the three-phase contact angle between a water droplet and pellets prepared with HA-P precipitated using acetic acid (Figure 25 A, B, and C) and citric acid (Figure 25 D, E, and F), at HA concentrations of 4, 7, and 10 g/L.

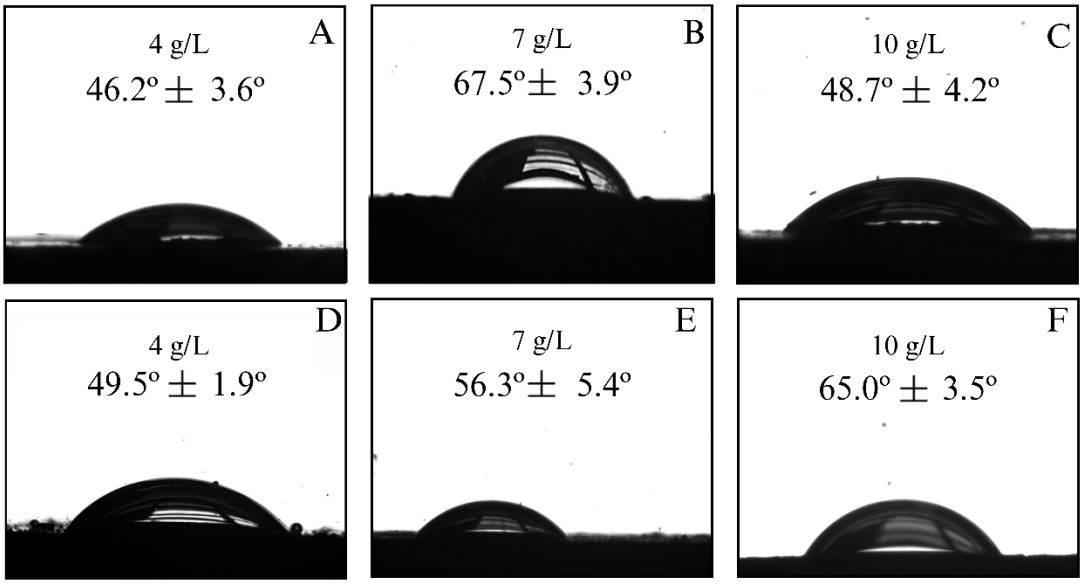

Figure 25 - Three-phase contact angle with the precipitating agents acetic acid (A, B, and C) and citric acid (D, E, and F) prepared with different acid humic concentrations (4, 7, and 10 g/L).

All contact angles were below 90°, indicating hydrophilic surfaces. However, both the precipitating agent and concentration affected the contact angle. In samples with acetic acid (Figure 25 A, B, and C), increasing the concentration from 4 to 7 g/L increased the contact angle, suggesting reduced affinity with water and a possible reorientation of less hydrophilic functional groups on the surface. However, at 10 g/L, the angle decreased again, indicating a return to higher hydrophilicity. This behavior may be related to changes in surface morphology and charge distribution after precipitation.

For samples precipitated with citric acid (Figure 25 D, E, and F), a gradual increase in contact angle was observed as particle concentration increased. This behavior may be related to how citric acid, a tricarboxylic acid, interacts with HA. It promotes the exposure of carboxylic groups, increasing the negative charge on the particle surface and making it more hydrophilic. However, as particle concentration increases, a structural reorganization occurs, promoting surface packing and compaction, which reduces the availability of exposed hydrophilic groups, limiting interaction with water and resulting in increased contact angle [55,56,60].

Interfacial tension measures the energy required to increase the contact area between two immiscible liquids or between a liquid and a solid surface [61]. Figure 26**Figure *26*** - Interfacial tension over time of water or HA-P precipitated with acetic acid and citric acid at humic acid concentrations of 4, 7, and 10 g/L in sweet almond oil. shows the variation in interfacial tension over time for different systems containing water and HA-P precipitated with acetic and citric acids at concentrations of 4, 7, and 10 g/L in a sweet almond oil medium.

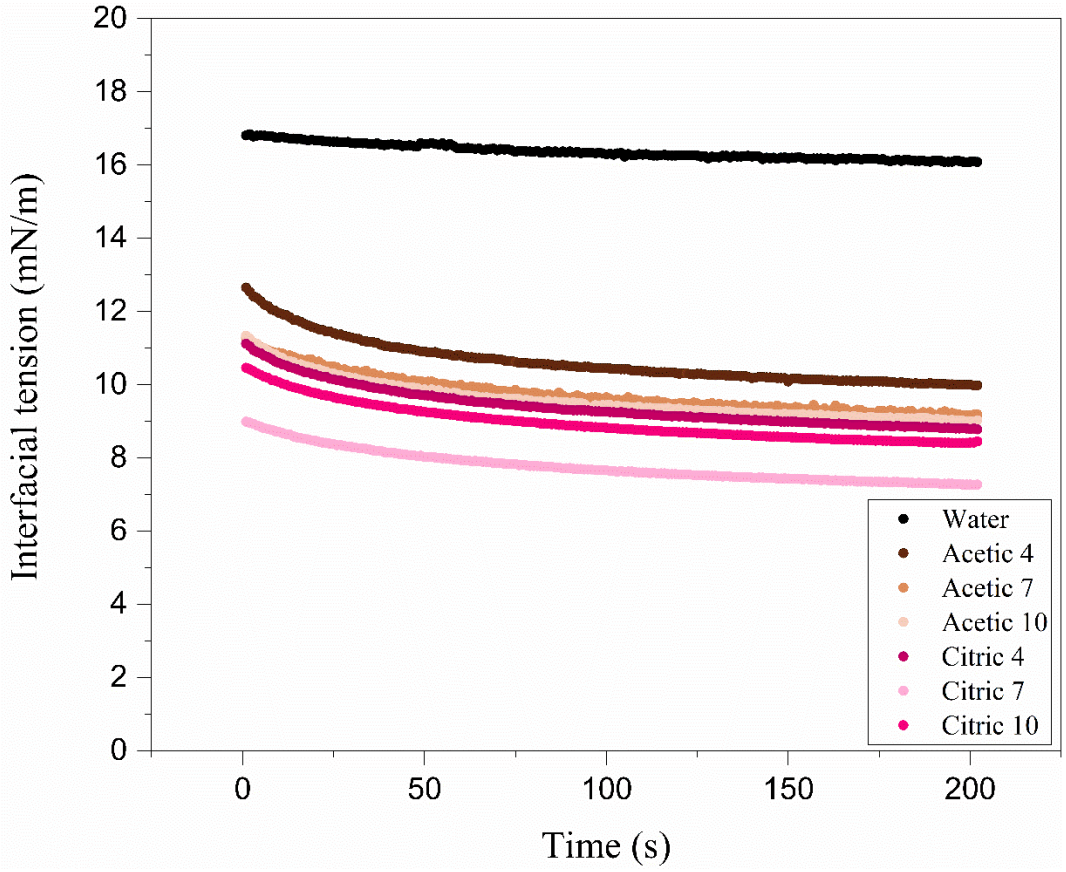

Figure 26 - Interfacial tension over time of water or HA-P precipitated with acetic acid and citric acid at humic acid concentrations of 4, 7, and 10 g/L in sweet almond oil.

The curve for water, represented by the black line, showed the highest interfacial tension compared to the others, suggesting that HA-P reduced the interfacial tension between water and sweet almond oil. Furthermore, HA-P precipitated with citric acid had lower interfacial tension than those with acetic acid. The structural differences between citric and acetic acids can explain this difference. Specifically, citric acid is a tricarboxylic acid, meaning it has three ionizable carboxyl groups, which gives it greater capacity for interaction with carboxylic and phenolic groups in HA. These interactions promote greater exposure of hydrophilic groups on the particle surface, increasing affinity with the aqueous phase and reducing interfacial tension [55,62]. On the other hand, acetic acid is a monocarboxylic acid with limited capacity to interact with HA functional groups, resulting in less modification of HA's surface and, therefore, higher interfacial tension compared to citric acid [55,62].

The observed behavior indicated that the type of precipitating agent directly influenced the ability of HA-P to reduce interfacial tension and, consequently, their Pickering stabilizing potential. Besides this, the HA concentration also played an essential role in the interfacial

tension. For both agents, as the concentration of particles increases, the interfacial tension decreases. This behavior is related to the greater availability of particles for migration and adsorption at the interface, favoring interfacial coverage and reducing the free energy of the interface. At higher concentrations, such as 7 and 10 g/L, the particles form a denser physical barrier between the phases, minimizing direct contact between water and oil molecules, which results in a decrease in interfacial tension [26].

Pickering emulsions were produced using the HA-P precipitated with acetic acid (Figure 27) and citric acid (Figure 28), using sweet almond oil as the oil phase at a 50% oil volume fraction.

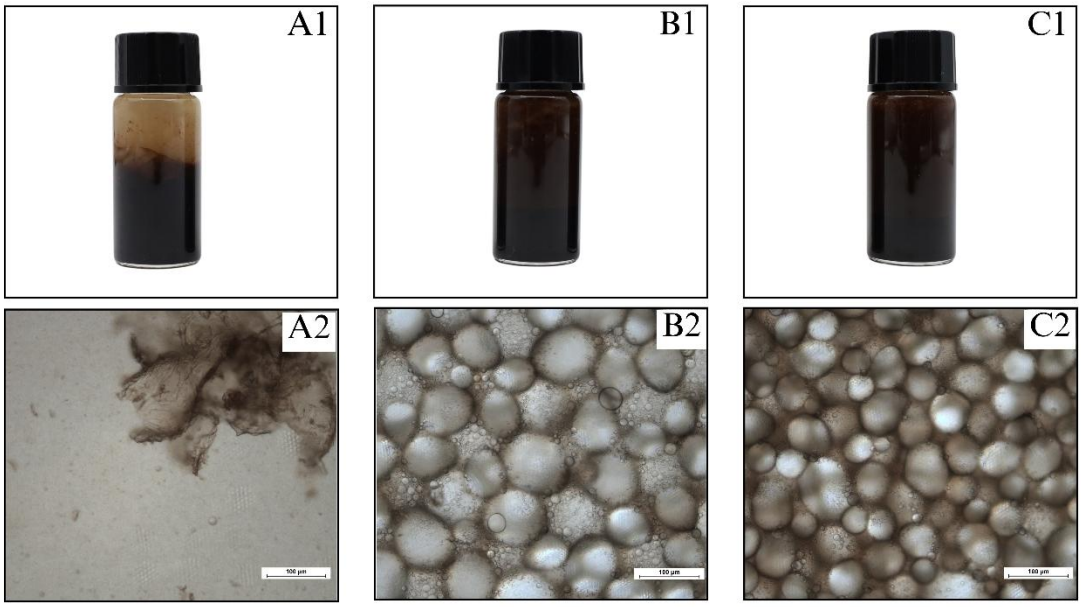

Figure 27 - Photo of Pickering emulsions (A1, B1 and C1) and corresponding optical microscopy (A2, B2 and C2) prepared with HA-P precipitated with acetic acid at different humic acid concentrations. A1 and A2: 4 g/L humic acid; B1 and B2: 7 g/L; C1 and C2: 10 g/L. Microscopy magnification of 100x.

For the samples where acetic acid was used as the precipitating agent, the emulsion prepared with HA-P at 4 g/L showed phase separation, with a clear serum on top and a dark brown emulsified phase. Furthermore, no droplets were detected under microscopy, revealing that no emulsion was formed. In contrast, the emulsions prepared with HA-P at 7 and 10 g/L were similar, showing a dark brown serum and an emulsified dark brown layer, and round and concentrated oil droplets were observed.

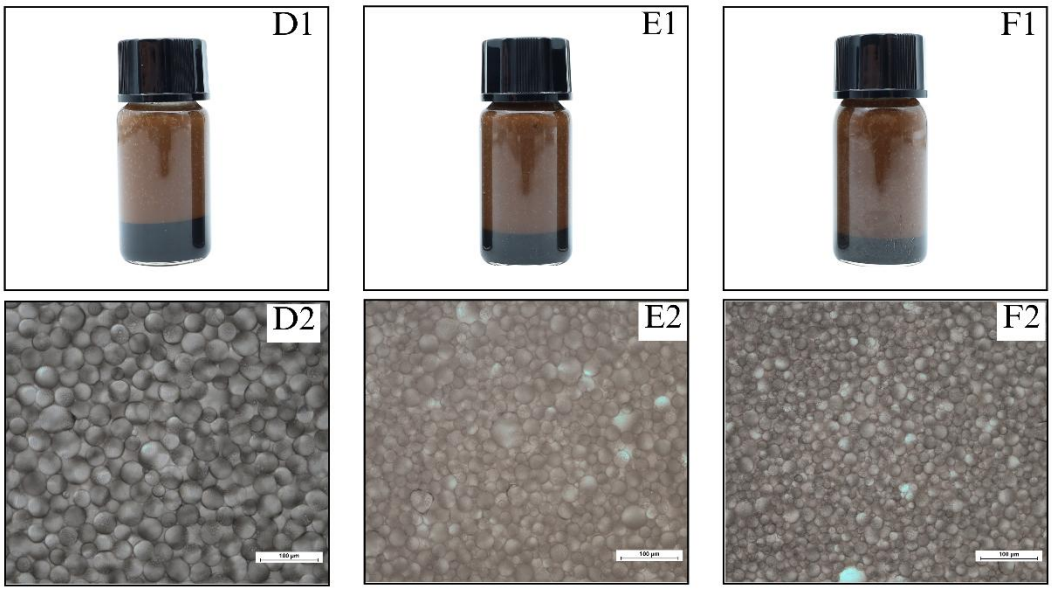

Figure 28 - Photo of Pickering emulsions (D1, E1 and F1) and corresponding optical microscopy (D2, E2 and F2) prepared with HA-P precipitated with citric acid at different humic acid concentrations. D1 and D2: 4 g/L humic acid; E1 and E2: 7 g/L; F1 and F2: 10 g/L. Microscopy magnification of 100x.

In contrast, the emulsions had similar visual aspects for the samples where citric acid was used as the precipitating agent (Figure 28), revealing a dark brown serum and a lighter brown emulsified layer. For all HA concentrations, emulsions showed smaller droplet sizes than those prepared with HA-P with acetic acid, revealing rounded and well-defined shapes.

Figure 29 shows the EL of the prepared emulsions over 45 days of storage. The samples followed a similar pattern from day 1 to 7, with a slight decrease in the EL. From day 7 to 45, all sample's EL values remained stable except for Citric 10. Still, this latter sample exhibited the largest EL compared to the other emulsions, exceeding 77%. Furthermore, it was observed that increasing the HA concentration from 4 to 10 g/L increased the EL for both types of acids. The results indicate that the percentage of EL in Pickering emulsions was directly related to the ability of HA-P to efficiently adsorb and cover the oil droplet interface. This interfacial coverage is essential for the system's stability, as it prevents phenomena such as coalescence and phase separation. Similar observations were reported by Sharkawy [49] in studies with Pickering emulsions stabilized by chitosan/gum Arabic nanoparticles.

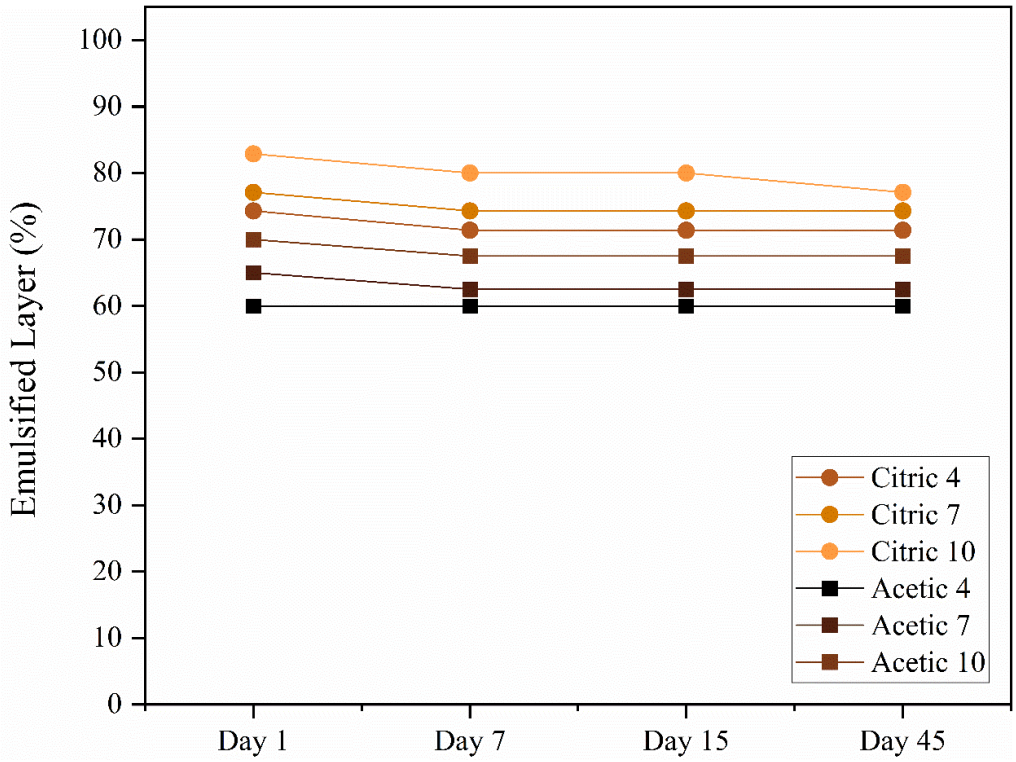

Figure 29 - Emulsified layer of Pickering emulsions produced with HA-P precipitated with acetic and citric acid at humic acid concentrations of 4, 7, and 10 g/L.

Based on the results, citric acid was selected as the ideal precipitating agent for obtaining HA-P at a HA concentration of 10 g/L. More specifically, these particles exhibited a zeta potential of -35.1 mV, indicating high electrostatic stability and low aggregation tendency. Additionally, these particles had nanometric sizes (73.9 nm), contributing to greater surface area for interfacial interactions. Wettability was also improved, with contact angles below 90°, demonstrating greater affinity with the aqueous phase and higher stabilization potential for O/W emulsified systems. Finally, the emulsions produced with these particles showed the largest EL, exceeding 77% after 45 days of storage. Therefore, the HA-P particles prepared with 10 g/L of HA and precipitated with citric acid were selected for further studies.

4.5 Characterization of the Optimized HA particle

Figure 30 shows a photograph of HA-P prepared with 10 g/L HA and precipitated with citric acid. These dark brown particles had an average size of 73.9 ± 9.7 nm and a zeta potential of -35.1 ± 1.3 mV.

Figure 30 - Photo of HA-P with 10 g/L.

To quantify HA-P yield, a dialysis process was carried out, as illustrated in Figure 31, where Figure 31 A corresponds to the beginning of the procedure, right after the water change in the medium, and Figure 31 B after a few hours of dialysis.

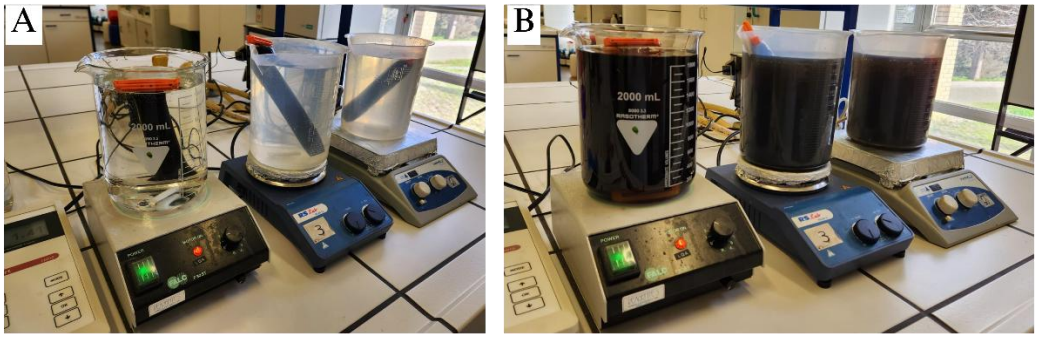

Figure 31 - Photo of the dialysis procedure: (A) after changing the medium water and (B) after a few hours.

The dark color of the water in Figure 31 B indicated the presence of soluble organic substances that have crossed the dialysis membrane, most likely fulvic acids [42]. Fulvic acids, unlike HAs, are soluble in water throughout the pH range and have a lower molecular weight. For this reason, during the dialysis step, fulvic acid is expected to cross the membrane and migrate to the external medium. At the same time, HA-P, which has a higher molecular weight and forms colloidal aggregates or particles, remains retained in the dialysis bag [42,44,50,63].

This selective separation allows the HA-P to be purified, removing fulvic fractions and residual salts to quantify the particle yield, which was calculated according to Equation (4). The yield of HA-P, calculated based on the dry mass recovered after dialysis in relation to the initially used soluble fraction, was 31.3%. This value aligns with the expected fractionation behavior, as only part of the soluble organic matter present in the initial fraction has a chemical structure suitable for forming HA-P after acidification.

Figure 32 shows the TEM images of HA-P. In both images, it was observed that HA-P particles are irregular and tend to form aggregates. The different magnifications revealed distinct structural details. At 80,000× magnification (Figure 36 A), the aggregates appeared less dense, with greater dispersion between particles. In contrast, at 100,000× magnification (Figure 36 B), the aggregates are more compact and overlapping, suggesting regions of higher electron density. The difference in contrast and density between the images may be related to the sample's heterogeneity and the effects of the TEM preparation process. As the samples were dried, part of the aggregation observed is likely due to this, which does not necessarily reflect the colloidal behavior of the particles in an aqueous medium.

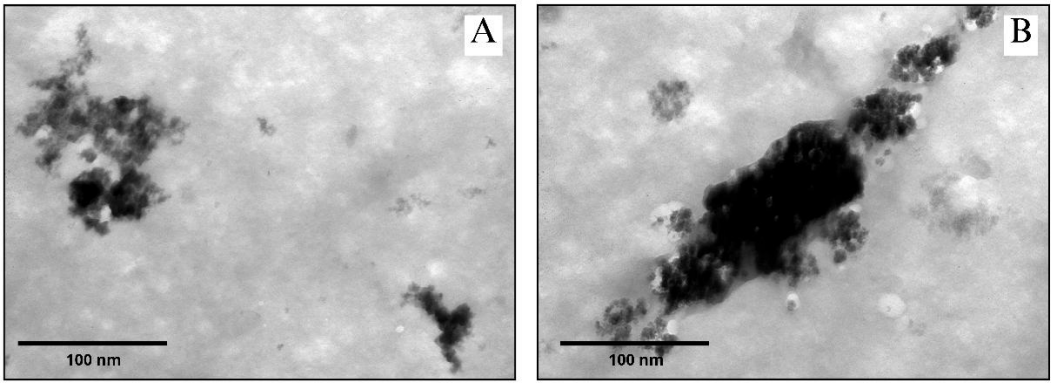

Figure 32 - TEM images of 10 g/L HA-P at magnifications of (A) 80,000x and (B) 100,000x.

4.6 Stabilization mechanism of HA-P in emulsion structure

An emulsion consisting of the optimized particle system and an oil volume percentage of 50% was prepared to analyze the particle distribution in the emulsion microstructure and confirm the type of emulsion formed. Confocal laser scanning microscopy (CLSM) was performed, where the emulsions were stained with the hydrophobic dye Nile Red. In Figure 33, the Nile Red dye is red, while the HA-P is blue due to its autofluorescence. The CLSM analysis showed that the HA-P were predominantly in the continuous aqueous phase, promoting a network stabilization mechanism. The formation of a particle network in the continuous phase can play an important role in restricting droplets' movement, contributing to an increase in the

viscosity of the system and enhancing emulsion stability, while at the same time reducing undesired phenomena such as aggregation and coalescence [40].

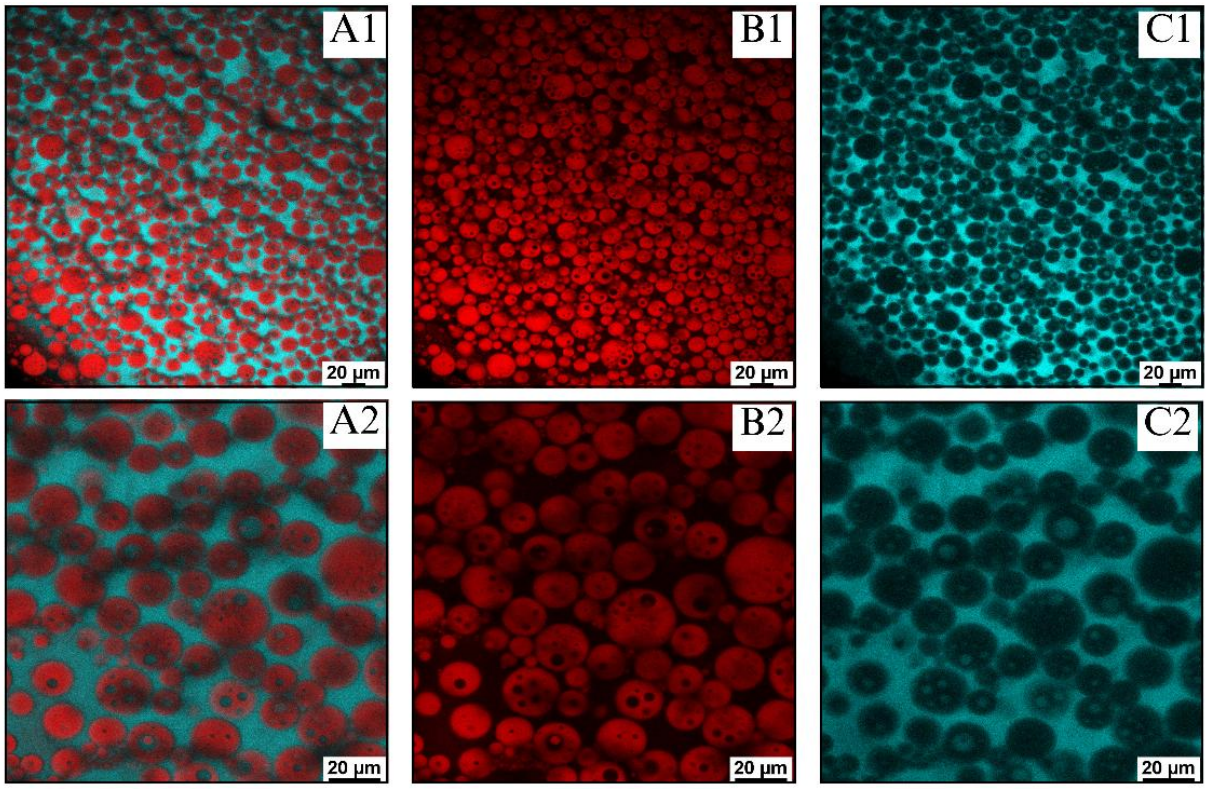

Figure 33 - Confocal microscopy images of emulsion stabilized with HA-P with 50% oil phase. A1 and A2 show the overlapped images, B1 and B2 show the fluorescence of Nile Red, and C1 and C2 show the autofluorescence of HA-P. Images were made with 40x magnification (A1, B1 and C1) and 60x magnification (A2, B2 and C2).

Upon further magnification, small spherical structures inside oil droplets were observed. These blue structures indicate that HA-P was possibly incorporated inside the oil droplets during emulsification. These internal structures were also visible in the optical microscopy image (Figure 34). Therefore, the observed results suggest forming a double emulsion system of water-in-oil-in-water (W/O/W) type made with only one step. The observed behavior may be related to the composition of the HA-P dispersion (produced using the HA soluble fraction in NaOH), which is composed of different HA fractions, namely fulvic acid and HA-P as perceived during the dialysis experiment. This was also observed for an emulsion system with a higher oil volume fraction (62.5%). Therefore, the formation of the double emulsion was independent of the oil volume percentage (Figure A 1 of Appendix A).

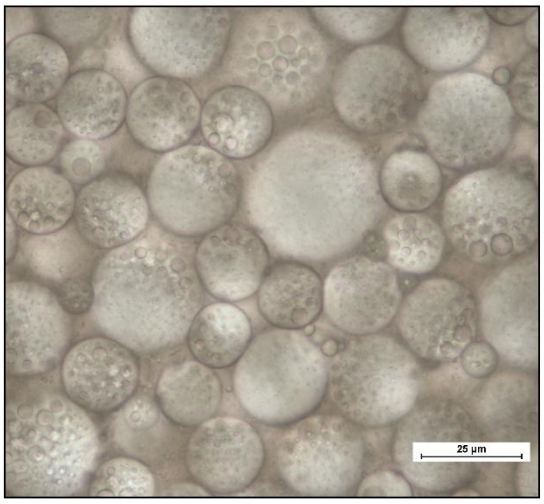

Figure 34 - Optical microscopy of the emulsion stabilized with HA-P with 50% oil phase (400x magnification).

4.7 Effect of oil volume fraction on emulsion properties

To study the effect of the oil volume fraction in emulsion preparation, HA-P prepared with HA concentration of 10 g/L and precipitated with citric acid was homogenized with sweet almond oil at different oil volume fractions: 50% (E-50), 55% (E-55), 60% (E-60), 65% (E-65), and 70% (E-70), as shown in Figure 35. The E-50 sample exhibited a dark brown serum and a brown emulsion. Emulsions E-55, E-60, and E-65 showed a light brown color and dark brown serum. In contrast, E-70 presented a dark brown emulsified phase and dark brown serum, with visibly large droplets observable to the naked eye, indicating a significant increase in droplet size.

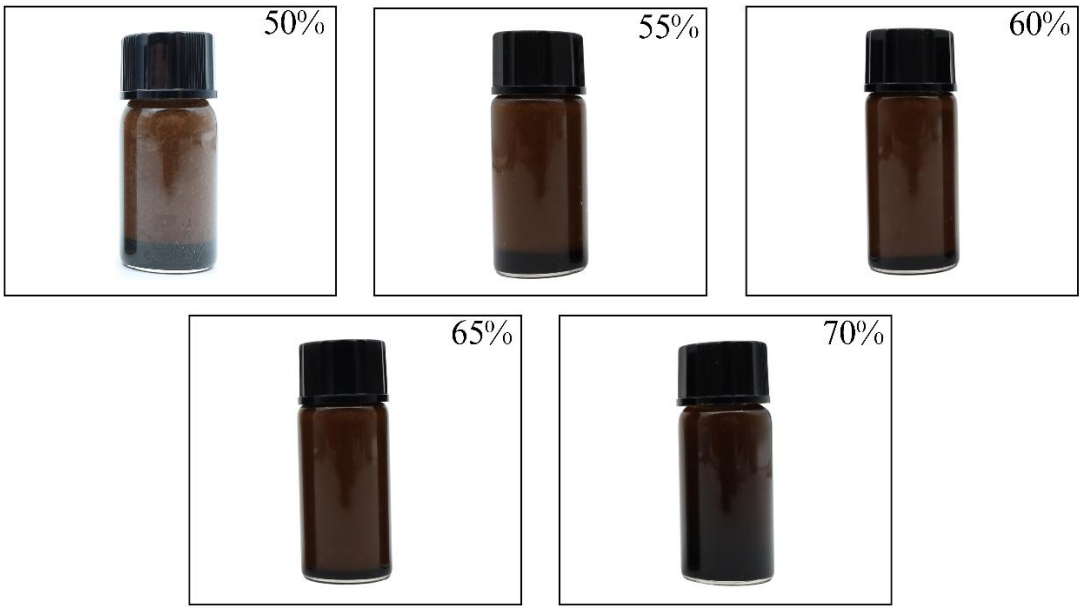

Figure 35 - Photo of Pickering emulsions stabilized with HA-P at different oil volume percentages.

The optical microscopy images (Figure 36) of the emulsions revealed that as the oil phase content increased, the average droplet size tended to grow.

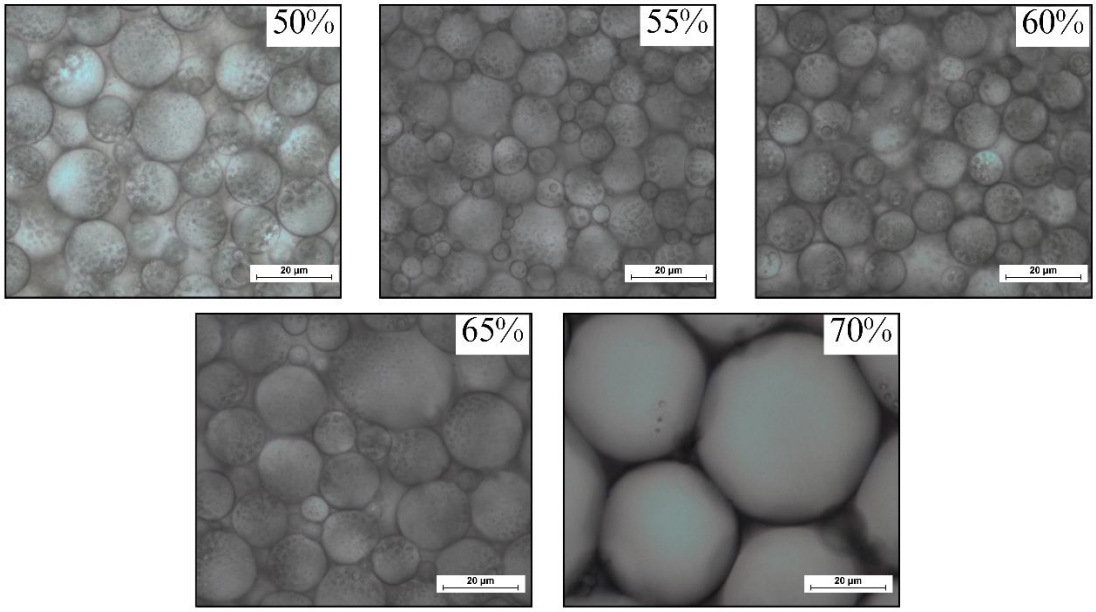

Figure 36 - Optical microscopy of Pickering emulsions stabilized with HA-P at different oil volume percentages (400 x magnification).

E-50 exhibited a relatively uniform distribution with smaller and well-stabilized droplets. In E-55, a relatively homogeneous distribution is still maintained. This trend becomes more evident at higher oil contents (E-60 and E-65), where a high droplet concentration and droplets with heterogeneous sizes are observed. There are also signs of coalescence in some areas, which suggests that there are not enough particles to stabilize the emulsions in response to the increase in the volume fraction of the oil phase. Furthermore, E-70 showed significantly larger and irregular droplets, with clear signs of coalescence, indicating reduced emulsion stability. This may be related to the limited stabilizing capacity of the solid particles in the system, which, at higher oil concentrations, become insufficient to effectively cover the entire oil/water interface [49]. These results indicate that the stability and structure of Pickering emulsions are highly dependent on the O/W ratio and the availability of particles for interfacial coverage. Furthermore, the presence of small droplets in the oil droplets was observed for E-50, E-55, E-60, and E-65 (Figure 36), suggesting that for these oil volume fractions, emulsions of the W/O/W type were formed.

Figure 37 shows the stability of the EL of the emulsions over 30 days of storage. The emulsions with lower oil concentrations (E-50 and E-55) presented lower EL. The E-60 emulsion demonstrated good performance, maintaining an EL of 92.5% over the entire stored period. The E-65 emulsion showed the highest EL of 95%, maintained throughout the evaluation period, indicating the most efficient system stabilization. On the contrary, the E-70 emulsion showed a slight decrease in the EL after 7 days, remaining stable from day 15 onward. Although some stability was maintained over time, the data suggested that this concentration represents the limit of the system's stabilizing capacity. These results indicate that intermediate to high oil concentrations, especially 65%, promoted the formation of more stable emulsions over time, likely due to a more efficient packing of the oil droplets through the HA-P particles.

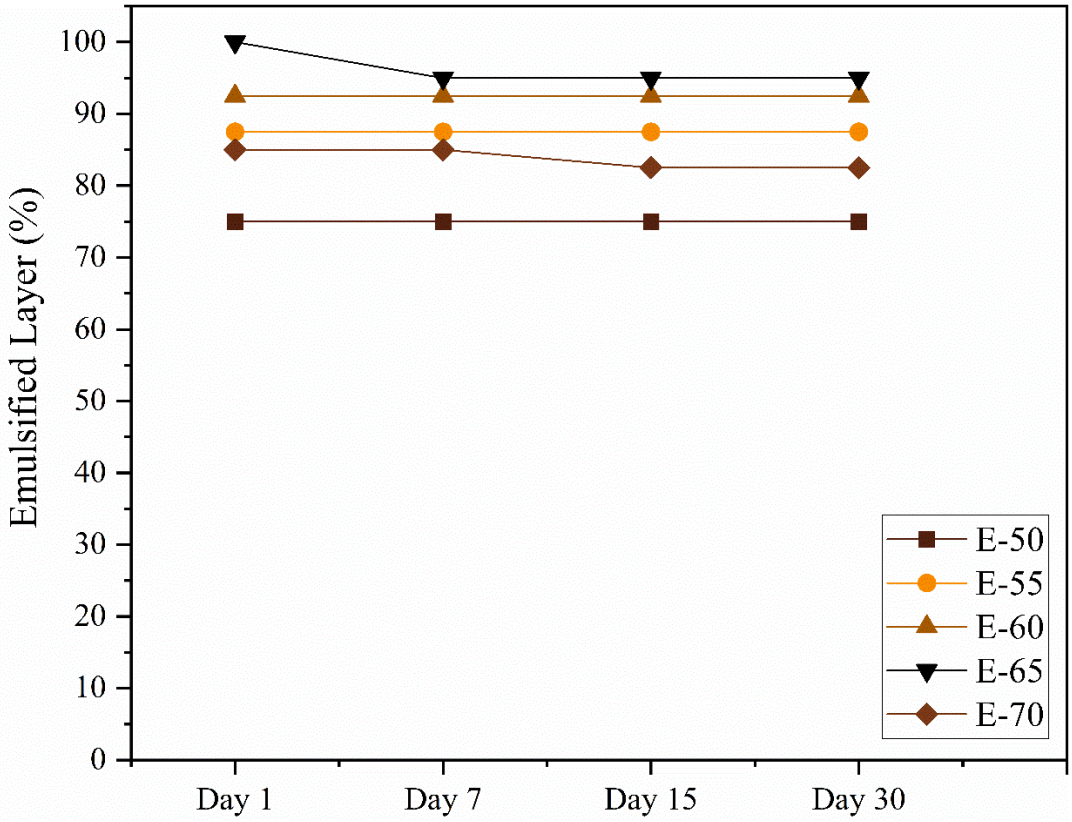

Figure 37 - Emulsified layer of Pickering emulsions stabilized with HA-P at different oil volume percentages over time.

Table 4 presents the average droplet diameters D[4,3] obtained after 1 and 30 days of storage, as well as the emulsion instability index (EII) of the emulsion systems. The EII represents the rate of change in droplet size over time and is a direct indication of the stability of the system. Higher EII values reflect greater emulsion instability, which is associated with the occurrence of processes such as droplet aggregation or coalescence. According to the

results, formulations E-50 and E-55 showed EII values between 0.5 and 5, indicating moderate instability, which suggests possible flocculation or partial coalescence of droplets during the storage period. Emulsion E-60 showed the lowest absolute variation in droplet size, associated with an EII of 0.0, classifying it as highly stable. Emulsion E-65 demonstrated satisfactory stability with an EII of 0.2. The slight increase in average droplet size did not significantly compromise the system's stability, and the data aligned with visual and microscopic analyses previously described, which indicate good cohesion and absence of coalescence. On the other hand, E-70 showed the largest droplets among all formulations, indicating a less stable structure. Although the EII still classified it as moderately stable, the large droplet size and broad size distribution observed in Figure 38 indicate a system more prone to instability.

Table 4 - Average droplet size D [4,3] of Pickering emulsions stabilized with HA-P at different oil volume percentages.

Emulsion	**D [4,3] (μm)**		**EII**
	Day 1	**Day 30**	
E-50	34.3 ± 0.3	37.1 ± 0.1	2.5
E-55	36.3 ± 0.2	41.6 ± 1.5	4.4
E-60	36.4 ± 0.2	36.3 ± 0.1	0.0
E-65	44.2 ± 0.3	44.5 ± 1.1	0.2
E-70	122.4 ± 2.7	123.2 ± 2.3	0.2

Figure 38 shows the volume-based droplet size distribution of Pickering emulsions with different oil concentrations, evaluated after 1 and 30 days of storage. The oil proportion in the formulation strongly influences droplet size and emulsion stability over time. Therefore, intermediate oil concentrations, particularly between 60 and 65%, showed the best performance in terms of stability and droplet size control.

Based on the parameters analyzed, the E-65 formulation was considered the most suitable for forming stable Pickering emulsions using HA-P as stabilizers. This emulsion showed uniform and intermediate droplet distribution and maintained an EL of 95% without significant variations over 30 days of storage. The optimized combination of oil content and solid particle concentration promoted efficient interfacial coverage, which can prevent droplet coalescence and flocculation. This structural balance gave the system high physicochemical stability, highlighting the E-65 formulation as the most promising emulsion system to proceed with further investigation to evaluate its potential for cosmetic applications.

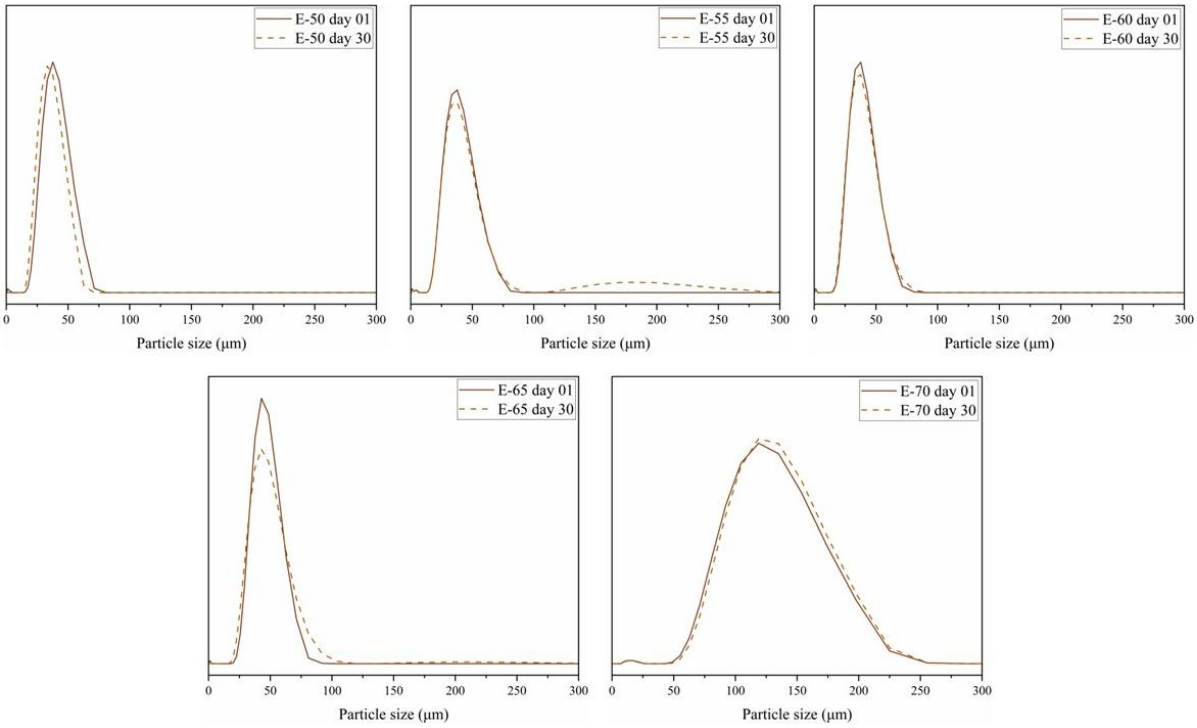

Figure 38 – Droplet size volume distribution of Pickering emulsions prepared with different oil volume percentages.

4.8 Characterization of optimized emulsion for cosmetic application

The optimized emulsion formulation (E-65), stabilized with HA-P and a 65% sweet almond oil volume fraction, was analyzed regarding its potential for cosmetic application. Considering the sensorial properties, this innovative formulation could be considered as an alternative facial mask. Therefore, the color of HA-65 and of a commercial facial mask containing carbon (Garnier PureActive) was analyzed. Additionally, the color of HA-P (10 g/L) was also determined for comparison purposes (Table 5).

Table 5 - Color parameters of the optimized emulsion, 10 g/L HA-P and commercial facial mask.

Sample	L*	a*	b*	RGB color
HA-P 10 g/L	20.94	1.18	-0.67	
E-65	26.80	4.61	5.43	
Commercial facial mask	31.86	0.89	-2.22	

The emulsion E-65 exhibited a brown color with an intermediate lightness, being lighter than the isolated particles and darker than the commercial mask. Regarding the a* parameter, E-65 showed a more intense reddish hue in contrast to the lower values observed for the other samples. For the b* parameter, the emulsion stood out with a positive shift (5.43), indicating a yellowish tone, unlike HA-P and the commercial mask, which presented bluish tones. This “earthy” coloration reinforces the natural character of the formulation. It may contribute to the sensory acceptance of the final product, demonstrating that emulsification enhanced the visual appeal of the HA formulation. The intense color of HA-P and the resulting emulsion E-65 is attributed to the inherently dark, nearly black hue of raw HA. In contrast, the coloration of the commercial facial mask is due to the presence of activated charcoal in its composition, which imparts the characteristic dark gray tone.

Figure 39 presents the percentage of antioxidant activity inhibition as a function of the concentration of the Pickering emulsion, E-65, at different concentrations. The results indicated a concentration-dependent behavior. Specifically, at lower concentrations, ranging from 0.005 to 0.5 mg/mL, no significant antioxidant activity was observed, with inhibition values equal to zero. However, from the concentration of 1 mg/mL, the emulsion showed an increase in antioxidant activity, reaching 14.0% inhibition, and at a concentration of 2 mg/mL, the value remained similar (14.8%). This behavior suggests that the antioxidant efficacy of the emulsion depends on the presence of a critical minimum concentration of HA active compounds capable of scavenging free radicals, which may be linked with the availability of HA functional groups

at the interface. Since the DPPH radical scavenging is a colorimetric assay and requires a fully dissolved system, it was not possible to test higher emulsion concentrations due to the emulsion's dark color and the difficulty of dissolving it at higher concentrations in the solvent. Nevertheless, the results support the potential of HA as an antioxidant agent in cosmetic formulations, particularly when incorporated into systems that maintain its stability and functional availability, such as Pickering emulsions. Further analyses are needed to fully confirm its antioxidant capacity.

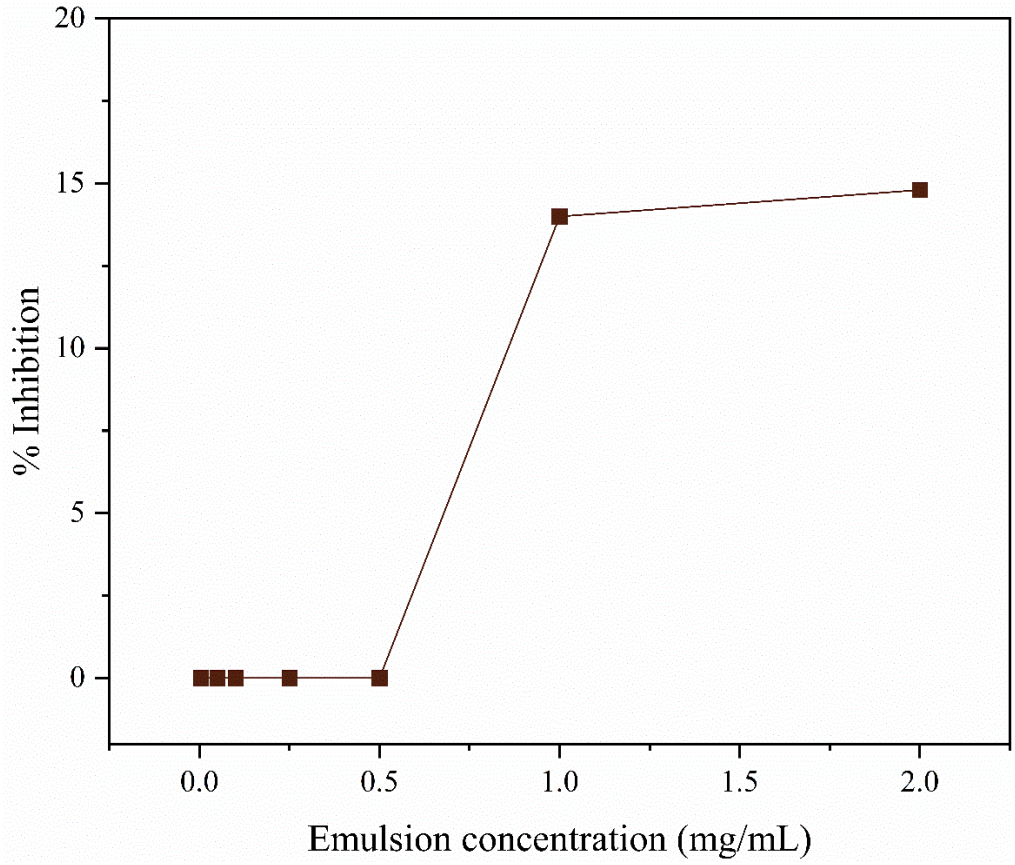

Figure 39 – Inhibition percentage of DPPH radical as a function of the concentration of Pickering emulsion (E-65).

The rheological behavior of the emulsions was analyzed based on the viscosity (Figure 40) and frequency sweep tests (Figure 41). The rheology of Pickering emulsions is associated with their internal structure, physical stability, and composition, and is mainly influenced by the presence of solid particles and their interparticle interactions [40].

Figure 40 shows that, as the shear rate increased, the viscosity of Pickering emulsions decreased, describing a shear-thinning non-Newtonian fluid [40,64]. This rheological profile is common in cosmetic formulations, such as face masks, and it is desirable because it facilitates

spreading on the skin, promotes better coverage, and provides a more pleasant sensory experience during use [64].

Figure 41 shows the measurement of the frequency sweep, in which a gel-like behavior was observed for the sample since the storage modulus (G') remained greater than the loss modulus (G'') throughout the frequency range evaluated. According to Cefali et al. [65], O/W emulsions that behave like a gel can preserve their internal structure, avoiding deformation or phase separation during storage in packaging.

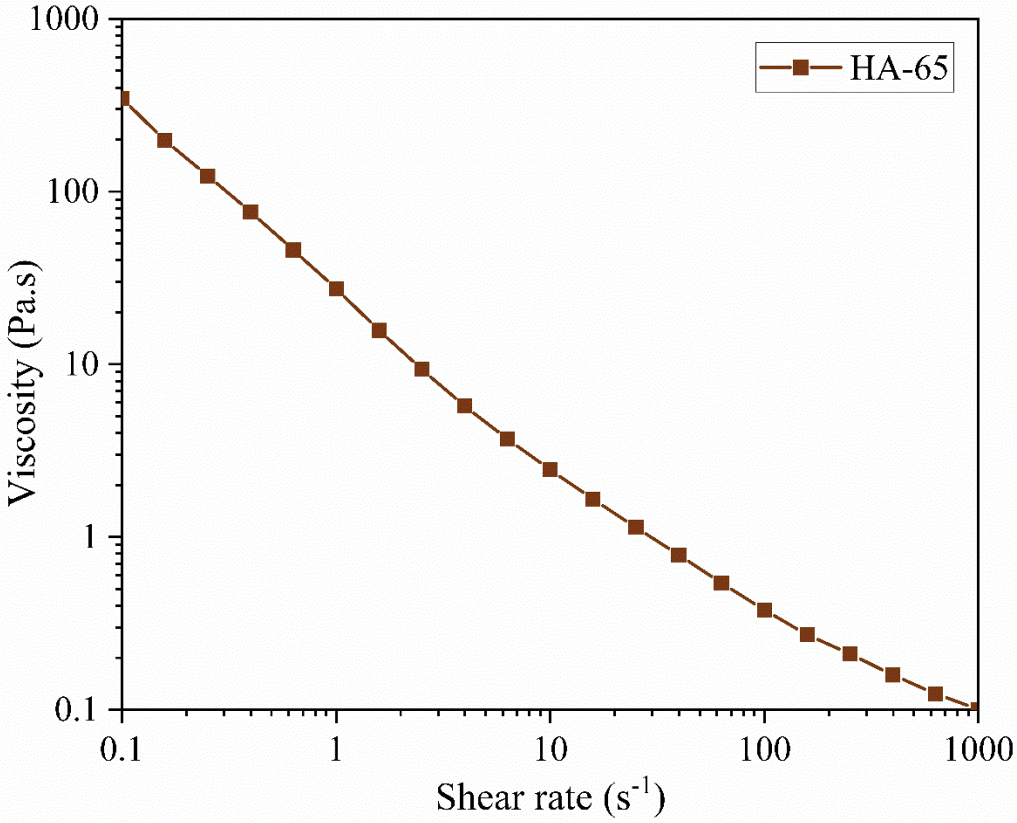

Figure 40 - Rheology of the Pickering emulsion: apparent viscosity versus shear rate.

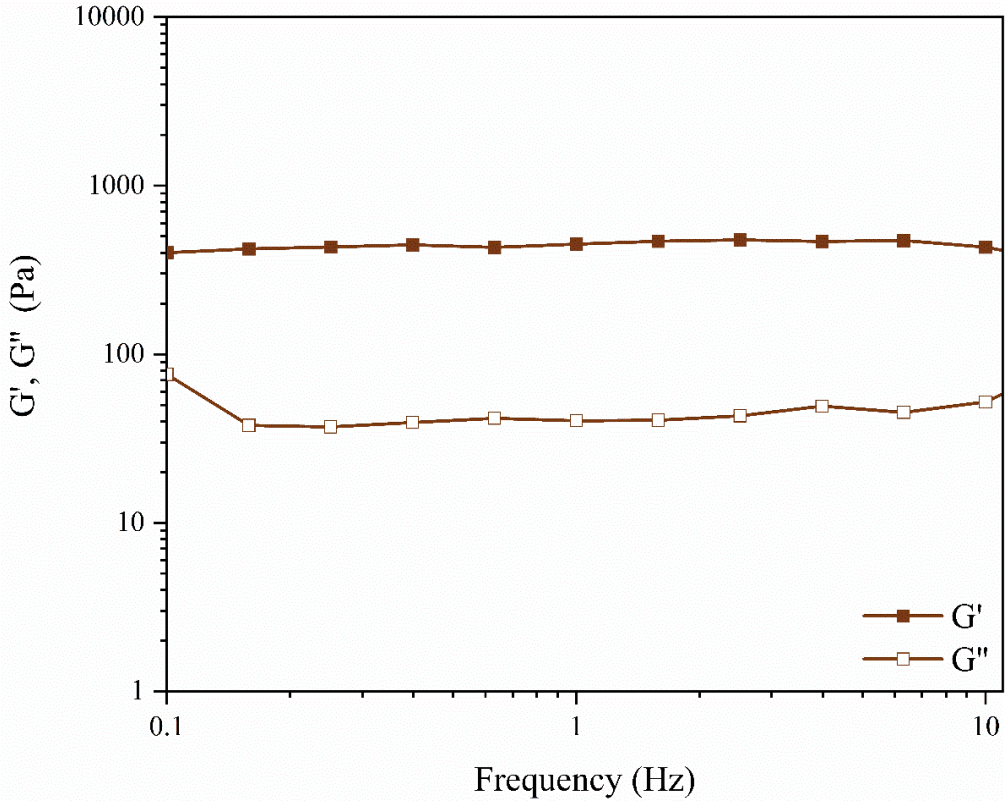

Figure 41 - Rheology of Pickering emulsions of storage (G′) and loss (G″) modulus versus angular frequency.

Texture analysis has proven to be an effective tool for evaluating the effect of ingredients on formulation performance and for quality control. These tests provide relevant information about the product's structure, which can directly impact its stability, shelf life, sensory properties, and behavior during processing [66].

Table 6 and Table 7 describe, respectively, the values obtained by the Backward Extrusion method and Spreadability Test method for the optimized emulsion and commercial face mask. The comparison between the optimized emulsion and the commercial face mask showed differences in textural and sensory properties, mainly attributed to the composition and presence of particles such as activated charcoal in the commercial formulation. In the Back Extrusion test, it was observed that the commercial mask showed significantly higher values for firmness (156.2 ± 2.4 g) and consistency (2382.9 ± 125.6 g.s) compared to the optimized emulsion, which showed firmness of 20.9 ± 0.5 g and consistency of 330.5 ± 5.5 g.s, indicating a much thicker and denser texture. In addition, the values for cohesiveness and work of cohesion were also higher for the commercial mask, suggesting greater resistance to deformation and a less flexible structure.

These results may be related to the presence of charcoal in the commercial mask's formulation. Charcoal contributes to increasing the product's viscosity and thickness, giving it

a denser feel during application. However, this greater firmness may be related to an abrasive sensation on the skin, especially in formulations with a high load of solid particles.

Table 6 - Texture parameters determined by the Backward Extrusion method for the commercial face mask and the optimized emulsion.

Parameters	Control - Commercial face mask	Optimized emulsion
Firmness (g)	156.2 ± 2.4	20.9 ± 0.5
Consistency (g.s)	2382.9 ± 125.6	330.5 ± 5.5
Cohesiveness (g)	-143.0 ± 5.1	-12.5 ± 0.5
Work of Cohesion (g.s)	-220.4 ± 10.5	-14.5 ± 0.9

In the Spreadability test, the same behavior was observed, namely the commercial mask showed much higher values for firmness (399.6 ± 13.7 g), work of shear (364.9 ± 16.8 g.s), and stickiness (-368.5 ± 12.9 g) compared to the optimized emulsion (firmness: 38.7 ± 3.7 g; work of shear: 33.7 ± 6.7 g.s; stickiness: -38.2 ± 4.7 g). These results indicate that, although the commercial mask has greater adhesiveness and resistance, the emulsion developed has a lighter and more pleasant texture, is easier to spread, less sticky, and potentially more comfortable during use.

Table 7 - Texture parameters determined by the Spreadability Test method for the commercial face mask and the optimized emulsion.

Parameters	Control - Commercial face mask	Optimized emulsion
Firmness (g)	399.6 ± 13.7	38.7 ± 3.7
Work of Shear (g.s)	364.9 ± 16.8	33.7 ± 6.7
Stickiness (g)	-368.5 ± 12.9	-38.2 ± 4.7
Work of Adhesion (g.s)	-99.4 ± 8.6	-9.1 ± 0.9

5 Conclusions and future work

5.1 Conclusions

This study aimed to develop an innovative cosmetic formulation based on Pickering emulsions stabilized by HA-P. The experimental steps allowed us to identify the ideal conditions for the production and application of these particles, aiming for greater stability and functionality of the particle dispersion.

Initially, it was determined that the combination of 0.5 M sodium hydroxide as the solvent and 0.5 M citric acid as the precipitating agent resulted in the most efficient particle formation. The concentration of 10 g/L of HA proved ideal for obtaining HA-P with an average size of 73.9 ± 9.7 nm, a zeta potential of -35.1 ± 1.3 mV, and a contact angle of 65° ± 3.5°, characteristics that favor the stabilization of oil/water interfaces in Pickering emulsion systems.

Regarding the emulsion production and optimization, it was possible to observe that the oil volume percentage had a significant influence on the stability, structure, and appearance of the system. Among the concentrations evaluated, the formulation containing 65% oil volume percentage showed the best performance, namely by the formation of a homogeneous emulsion, a stable coloration, a 95% EL after 30 days of storage, and an average droplet size of 44.2 ± 0.3 μm. It had a shear-thinning and gel-like behavior, presenting a light and pleasant texture, with easy spreadability and little stickiness. The antioxidant activity reinforced the functional potential of HA, not only as a physical stabilizer, but also as a bioactive agent of interest for dermocosmetic formulations.

Overall, the results obtained demonstrated the potential of HA as a multifunctional component in cosmetic formulations, being effective both in stabilizing Pickering emulsions and in delivering functional benefits. The formulation developed, especially for products such as face masks, represents a promising proposal within the trend of natural and sustainable cosmetics, offering an innovative and technically viable alternative for the industry. It is to highlight that that studies using humic acid as a stabilizer in Pickering emulsions are still very rare in the literature, and this was the first work conducted on this topic within the research group.

5.2 Future work

To further develop and optimize the proposed formulation, some suggestions could be tested in order to validate its efficacy, safety, and applicability in cosmetic applications:

- In vitro skin permeation assays using Franz diffusion cells, aimed at evaluating the penetration and release capacity of active compounds through the skin;
- Accelerated stability analysis using freeze–thaw cycling, to assess potential changes in color, consistency, pH, and phase separation;
- Biocompatibility and safety evaluation through cytotoxicity testing;
- Alternative antioxidant analyses to better confirm the antioxidant potential of the optimized emulsion.

REFERENCES

[1] McKinsey & Company, O mercado de beleza em 2023 um relatório especial sobre o estado da moda, (2023).

[2] L'Óréal, L'Oréal 2022 universal registration document, 2022.

[3] A.C.D. Martins, Caracterização da Inovação na Indústria Cosmética: Estudo de Caso L'Oréal, Instituto Universitário de Lisboa, 2020.

[4] C.M. Oliveira, Utilização de Produtos Naturais em Indústria Cosmética: Uma máscara para a idade, Universidade do Algarve, 2020.

[5] A. Sharkawy, M.F. Barreiro, A.E. Rodrigues, New Pickering emulsions stabilized with chitosan/collagen peptides nanoparticles: Synthesis, characterization and tracking of the nanoparticles after skin application, Colloids Surf A Physicochem Eng Asp 616 (2021). https://doi.org/10.1016/j.colsurfa.2021.126327.

[6] E. Guzmán, F. Ortega, R.G. Rubio, Pickering Emulsions: A Novel Tool for Cosmetic Formulators, Cosmetics 9 (2022) 68. https://doi.org/10.3390/cosmetics9040068.

[7] L. Ming, H. Wu, A. Liu, A. Naeem, Z. Dong, Q. Fan, G. Zhang, H. Liu, Z. Li, Evolution and critical roles of particle properties in Pickering emulsion: A review, J Mol Liq 388 (2023). https://doi.org/10.1016/j.molliq.2023.122775.

[8] Z. Islam, A. Tutar, Humic substances-versatile natural products: Properties & applications, in: Bulgaria, 2018. https://www.researchgate.net/publication/335526473.

[9] B. Dreno, E. Araviiskaia, E. Berardesca, T. Bieber, J. Hawk, M. Sanchez-Viera, P. Wolkenstein, The science of dermocosmetics and its role in dermatology, (2014). https://doi.org/DOI:10.1111/jdv.12497.

[10] I. Kurokawa, M. Kobayashi, Y. Nomura, M. Abe, D. Kerob, B. Dreno, The Role and Benefits of Dermocosmetics in Acne Management in Japan, Dermatol Ther (Heidelb) 13 (2023) 1423–1433. https://doi.org/https://doi.org/10.1007/s13555-023-00943-x.

[11] Z.D. Draelos, L. Wei, M. Sachdev, B.S.F. Bravo, V. Vachiramon, M. Jourdan, M. Kerscher, C. Delva, S. Leclerc-Mercier, International Consensus on Anti-Aging Dermocosmetics and Skin Care for Clinical Practice Using the RAND/UCLA Appropriateness Method, Journal of Drugs in Dermatology 23 (2024) 1337–1343. https://doi.org/10.36849/JDD.7798.

[12] B. Zegarska, L. Rudnicka, J. Narbutt, W. Barańska-Rybak, B. Bergler-Czop, E. Chlebus, M. Czarnecka-Operacz, J. Czuwara, A. Kaszuba, R. Nowicki, A. Owczarczyk-Saczonek, W. Placek, M. Sokołowska-Wojdyło, J. Szepietowski, Dermocosmetics in

dermatological practice. Recommendations of the Polish Dermatological Society. Part 1, Przegl Dermatol 110 (2023) 121–132. https://doi.org/10.5114/dr.2023.127834.

[13] N.C. Alves, Penetration of actives on the skin: a literature review, Revista Amazônia Science & Health (2015). https://doi.org/DOI:10.18606/2318-1419/amazonia.sci.health.v3n4p36-43.

[14] P.O. Santos, P.Y. Muyashiro, V.A. Silva, A Nanotecnologia em Formulação Cosmética, Centro Universitário das Faculdades Metropolitanas Unidas - FMU, 2015.

[15] T. Agostini, D. Silva, Ácido Hialurônico: princípio ativo de produtos cosméticos, n.d.

[16] G.M.S. Gonçalves, P.M.B.G.M. Campos, Aplicação de métodos de biofísica no estudo da eficácia de produtos dermocosméticos, Brazilian Journal of Pharmaceutical Sciences 45 (2009). https://doi.org/https://doi.org/10.1590/S1984-82502009000100002.

[17] P.G. Ferreira, D.O. Futuro, L.S.M. Forezi, F.C. Silva, V.F. Ferreira, Aqui tem Química: Parte VII. Tensoativos em Produtos Comerciais, (2022) 1–16. https://doi.org/http://dx.doi.org/10.21577/1984-6835.20220105.

[18] P.A. Almeida, Investigação e Desenvolvimento de tintas com emulsões Etilénicas vs Estireno Acrílicas vs Vinilo Acrílicas, 2019.

[19] M. Ferrari, M.S.C. Oliveira, A.K. Nakano, P.A. Rocha-Filho, Determinação do fator de proteção solar (FPS) in vitro e in vivo de emulsões com óleo de andiroba (Carapa guianensis), Revista Brasileira de Farmacognosia 17 (2007) 626–630. https://doi.org/https://doi.org/10.1590/S0102-695X2007000400023.

[20] R.M.L. Castro, Emulsão: uma revisão bibliográfica, Universidade Federal da Paraíba, 2014.

[21] L.M. Fidelis, Desenvolvimento, Avaliação e Classificação de Emulsões Cosméticas Óleo/Água, Universidade Federal de Uberlândia, 2020.

[22] D.B. Andrade, Influência da Composição da Fase Oleosa nas Propriedades Físico-Químicas de Emulsões Cosméticas Com e Sem Filtros Solares Orgânicos, Pontifícia Universidade Católica do Rio de Janeiro, 2022.

[23] L.M.D. Barranco, Nanopartículas de sílica funcionalizadas com grupos amônio e polímeros aniônicos para estabilização de emulsões Pickering contendo repelente de insetos, Pontifícia Universidade Católica do Rio de Janeiro, 2018.

[24] B. Guevara-Guerrero, C.A. Beltrán, J.C. Montero-Montero, M.P. Valdés-Restrepo, Encapsulação de compostos bioativos por emulsão Pickering: revisão, Revista

Colombiana de Investigaciones Agroindustriales 10 (2022) 1–12. https://doi.org/10.23850/24220582.5005.

[25] G. Caldeira, G. Rodrigo, J. Joana, J. Ferreira, L. Stefany, FORMULAÇÃO E ELABORAÇÃO DE SHAMPOO SUBSTITUINDO TENSOATIVOS SULFATADOS POR TENSOATIVOS DE ORIGEM NATURAL, Centro Estadual de Educação Tecnológica Paula Souza, 2022.

[26] Y. Chevalier, M.A. Bolzinger, Emulsions stabilized with solid nanoparticles: Pickering emulsions, Colloids Surf A Physicochem Eng Asp 439 (2013) 23–34. https://doi.org/10.1016/j.colsurfa.2013.02.054.

[27] G.T. da Silva, Estudo da coalescência de gotas de óleo em água usando nanopartículas, Pontifícia Universidade Católica do Rio de Janeiro, 2018.

[28] C. Guida, PRODUÇÃO E CARACTERIZAÇÃO DE EMULSÕES PICKERING ESTABILIZADAS COM NANOPARTÍCULAS DE AMIDO DE MANDIOCA, Universidade Estadual de Campinas, 2021. https://orcid.org/0000-0003-1012-1845.

[29] A. Sharkawy, F. Barreiro, A. Rodrigues, Pickering emulsions stabilized with chitosan/gum Arabic particles: Effect of chitosan degree of deacetylation on the physicochemical properties and cannabidiol (CBD) topical delivery, J Mol Liq 355 (2022). https://doi.org/10.1016/j.molliq.2022.118993.

[30] C.G. Otoni, H.M.C. de Azeredo, NANOEMULSÕES POLIMÉRICAS, (n.d.).

[31] L.C. Ghirro, DESENVOLVIMENTO DE EMULSÕES PICKERING PARA APLICAÇÃO ALIMENTAR, Instituto Politécnico de Bragança, 2020.

[32] S.G.P. Peito, Nano and microparticle stabilized Pickering emulsions designed for therapeutic and cosmetic applications, Universidade de Coimbra, 2020.

[33] C. Albert, M. Beladjine, N. Tsapis, E. Fattal, F. Agnely, N. Huang, Pickering emulsions: Preparation processes, key parameters governing their properties and potential for pharmaceutical applications, Journal of Controlled Release 309 (2019) 302–332. https://doi.org/10.1016/j.jconrel.2019.07.003.

[34] F. Wu, J. Deng, L. Hu, Z. Zhang, H. Jiang, Y. Li, Z. Yi, T. Ngai, Investigation of the stability in Pickering emulsions preparation with commercial cosmetic ingredients, Colloids and Surfaces A 602 (2020). https://doi.org/https://doi.org/10.1016/j.colsurfa.2020.125082.

[35] D. Terescenco, N. Hucher, C. Picard, G. Savary, Sensory perception of textural properties of cosmetic Pickering emulsions, Int J Cosmet Sci 42 (2020) 198–207. https://doi.org/doi:10.1111/ics.12604.

[36] V. Calabrese, J.C. Courtenay, K.J. Edler, J.L. Scott, Pickering emulsions stabilized by naturally derived or biodegradable particles, (2018). https://doi.org/https://doi.org/10.1016/j.cogsc.2018.07.002.

[37] J. Frelichowska, M.A. Bolzinger, J.P. Valour, H. Mouaziz, J. Pelletier, Y. Chevalier, Pickering w/o emulsions: Drug release and topical delivery, Int J Pharm 368 (2009) 7–15. https://doi.org/10.1016/j.ijpharm.2008.09.057.

[38] J. Wang, H. Deng, Y. Sun, C. Yang, Montmorillonite and alginate co-stabilized biocompatible Pickering emulsions with multiple-stimulus tunable rheology, J Colloid Interface Sci 562 (2020) 529–539. https://doi.org/10.1016/j.jcis.2019.11.081.

[39] I. Capron, B. Cathala, Surfactant-free high internal phase emulsions stabilized by cellulose nanocrystals, Biomacromolecules 14 (2013) 291–296. https://doi.org/10.1021/bm301871k.

[40] G. Colucci, A. Ribeiro, M.B. Figueirêdo, J. Charmillot, A. Santamaria-Echart, A.E. Rodrigues, M.F. Barreiro, Lignin from aldehyde-assisted fractionation can provide light-colored Pickering emulsions through colloidal particles formed using alkaline antisolvent, Int J Biol Macromol 302 (2025). https://doi.org/10.1016/j.ijbiomac.2025.140534.

[41] M. Klučáková, M. Kalina, Composition, particle size, charge, and colloidal stability of pH-fractionated humic acids, J Soils Sediments 15 (2015) 1900–1908. https://doi.org/10.1007/s11368-015-1142-2.

[42] G. Chilom, A.S. Bruns, J.A. Rice, Aggregation of humic acid in solution: Contributions of different fractions, Org Geochem 40 (2009) 455–460. https://doi.org/https://doi.org/10.1016/j.orggeochem.2009.01.010.

[43] S. de M. Colombo, L.B.D.O. dos Santos, J.C. Masini, PROPRIEDADES ÁCIDO-BASE E DE COMPLEXAÇÃO DE ÁCIDOS HÚMICO E FÚLVICO ISOLADOS DE VERMICOMPOSTO, Quim. Nova 30 (2007) 1261–1266. https://doi.org/https://doi.org/10.1590/S0100-40422007000500039.

[44] B.A.G. Melo, F.L. Motta, M.H.A. Santana, Humic acids: Structural properties and multiple functionalities for novel technological developments, Materials Science and Engineering C (2015). https://doi.org/10.1016/j.msec.2015.12.001.

[45] California Association of Chemistry Teachers, What Is Humic Acid?, 1963.

[46] J.C.R. de Azevedo, J. Nozaki, Análise de Fluorescência de Substâncias Húmicas Extraídas da Água, Solo e Sedimento da Lagoa dos Patos - MS, Quim. Nova 31 (2008) 1324–1329. https://doi.org/https://doi.org/10.1590/S0100-40422008000600010.

[47] M.B. Agustin, P.A. Penttilä, M. Lahtinen, K.S. Mikkonen, Rapid and Direct Preparation of Lignin Nanoparticles from Alkaline Pulping Liquor by Mild Ultrasonication, ACS Sustain Chem Eng 7 (2019) 19925–19934. https://doi.org/10.1021/acssuschemeng.9b05445.

[48] B.A.G. Melo, F.L. Motta, M.H.A. Santana, PRODUÇÃO E CARACTERIZAÇÃO DE NANOPARTÍCULAS DE ÁCIDOS HÚMICOS POR NANOPRECIPITAÇÃO, in: Florianópolis, 2014.

[49] A. Sharkawy, M.F. Barreiro, A.E. Rodrigues, Preparation of chitosan/gum Arabic nanoparticles and their use as novel stabilizers in oil/water Pickering emulsions, Carbohydr Polym 224 (2019). https://doi.org/10.1016/j.carbpol.2019.115190.

[50] S.W. Cowling, Emulsions Stabilized by Humic Acids, Colorado School, 1991.

[51] G. Colucci, M. Gigli, M. Sgarzi, A.E. Rodrigues, C. Crestini, M.F. Barreiro, Modulation of physicochemical and antioxidant properties of Pickering emulsions using colloidal lignin particles based on kraft softwood and hardwood acetone fractions, Sep Purif Technol 347 (2024). https://doi.org/10.1016/j.seppur.2024.127570.

[52] D.J. McClements, J. Lu, L. Grossmann, Proposed Methods for Testing and Comparing the Emulsifying Properties of Proteins from Animal, Plant, and Alternative Sources, Colloids and Interfaces 6 (2022). https://doi.org/10.3390/colloids6020019.

[53] W. Brand-Williams, M.E. Cuvelier, C. Berset, Use of a Free Radical Method to Evaluate Antioxidant Activity, 1995. https://doi.org/https://doi.org/10.1016/S0023-6438(95)80008-5.

[54] C.I.S. Oliveira, Desenvolvimento de maioneses com “farinha de azeitona de mesa”: caracterização físico-química, atividade antioxidante e sensorial, 2020.

[55] F.L. Motta, B.A.G. Melo, M.H.A. Santana, Deprotonation and protonation of humic acids as a strategy for the technological development of pH-responsive nanoparticles with fungicidal potential, N Biotechnol 33 (2016) 773–780. https://doi.org/10.1016/j.nbt.2016.07.003.

[56] A.G.S. Prado, J. Pertusatti, A.R. Nunes, Aspects of Protonation and Deprotonation of Humic Acid Surface on Molecular Conformation, Article J. Braz. Chem. Soc 22 (2011) 1478–1483. https://doi.org/https://doi.org/10.1590/S0103-50532011000800011.

[57] A. Franzol, M.C. Rezende, Estabilidade de emulsões: um estudo de caso envolvendo emulsionantes aniônico, catiônico e não-iônico, Polimeros 25 (2015) 1–9. https://doi.org/10.1590/0104-1428.1669.

[58] R.A. Alvarez-Puebla, J.J. Garrido, Effect of pH on the aggregation of a gray humic acid in colloidal and solid states, Chemosphere 59 (2005) 659–667. https://doi.org/10.1016/j.chemosphere.2004.10.021.

[59] R. Angelico, C. Colombo, E. Di Iorio, M. Brtnický, J. Fojt, P. Conte, Humic Substances: From Supramolecular Aggregation to Fractal Conformation—Is There Time for a New Paradigm?, Applied Sciences (Switzerland) 13 (2023). https://doi.org/10.3390/app13042236.

[60] M. Klučáková, Size and charge evaluation of standard humic and fulvic acids as crucial factors to determine their environmental behavior and impact, Front Chem 6 (2018). https://doi.org/10.3389/fchem.2018.00235.

[61] K. Schroën, J. de Ruiter, C. Berton-Carabin, The importance of interfacial tension in emulsification: Connecting scaling relations used in large scale preparation with microfluidic measurement methods, ChemEngineering 4 (2020) 1–22. https://doi.org/10.3390/chemengineering4040063.

[62] M. Terashima, M. Fukushima, S. Tanaka, Influence of pH on the surface activity of humic acid: Micelle-like aggregate formation and interfacial adsorption, Colloids Surf A Physicochem Eng Asp 247 (2004) 77–83. https://doi.org/10.1016/j.colsurfa.2004.08.028.

[63] A. Ukalska-Jaruga, R. Bejger, G. Debaene, B. Smreczak, Characterization of soil organic matter individual fractions (Fulvic acids, humic acids, and humins) by spectroscopic and electrochemical techniques in agricultural soils, Agronomy 11 (2021). https://doi.org/10.3390/agronomy11061067.

[64] R. Rodrigues, J.C. Lobo, D.M. Ferreira, E. Senderowicz, M.A. Nunes, M.H. Amaral, R.C. Alves, M.B.P.P. Oliveira, Chemical and Rheological Characterization of a Facial Mask Containing an Olive Pomace Fraction, Cosmetics 10 (2023). https://doi.org/10.3390/cosmetics10020064.

[65] L.C. Cefali, J.A. Ataide, A.R. Fernandes, I.M. de O. Sousa, F.C. da S. Gonçalves, S. Eberlin, J.L. Dávila, A.F. Jozala, M.V. Chaud, E. Sanchez-lopez, J. Marto, M.A. D'ávila, H.M. Ribeiro, M.A. Foglio, E.B. Souto, P.G. Mazzola, Flavonoid-enriched plant-extract-loaded emulsion: A novel phytocosmetic sunscreen formulation with antioxidant properties, Antioxidants 8 (2019). https://doi.org/10.3390/antiox8100443.

[66] R. Rodrigues, J.C. Lobo, D.M. Ferreira, E. Senderowicz, M.A. Nunes, M.H. Amaral, R.C. Alves, M.B.P.P. Oliveira, Chemical and Rheological Characterization of a Facial Mask Containing an Olive Pomace Fraction, Cosmetics 10 (2023). https://doi.org/10.3390/cosmetics10020064.

APPENDIX A

Table A 1 - Size and zeta potential of HA-P produced at pH 5, 7, and 9.

Particles	Size (nm)	Zeta Potential (mV)
HA-P pH 5	5688.7 ± 486.9	-25.2 ± 0.8
HA-P pH 7	72.4 ± 2.3	-36.2 ± 2.8
HA-P pH 9	87.2 ± 12.9	-57.9 ± 4.0

Table A 2 - Size and zeta potential of HA-P prepared with humic acid concentrations of 4, 7 and 10 g/L and with the acetic acid and citric acid.

Humic acid concentration (g/L)	Precipitating agent	Size (nm)	Zeta Potential (mV)
4		267.8 ± 8.5	-18.8 ± 3.4
7	Acetic acid	66.7 ± 0.4	-49.7 ± 2.4
10		64.2 ± 6.7	-60.6 ± 1.7
4		90.4 ± 3.0	-44.5 ± 1.9
7	Citric acid	75.1 ± 3.7	-34.7 ± 6.3
10		73.9 ± 9.7	-35.1 ± 1.3

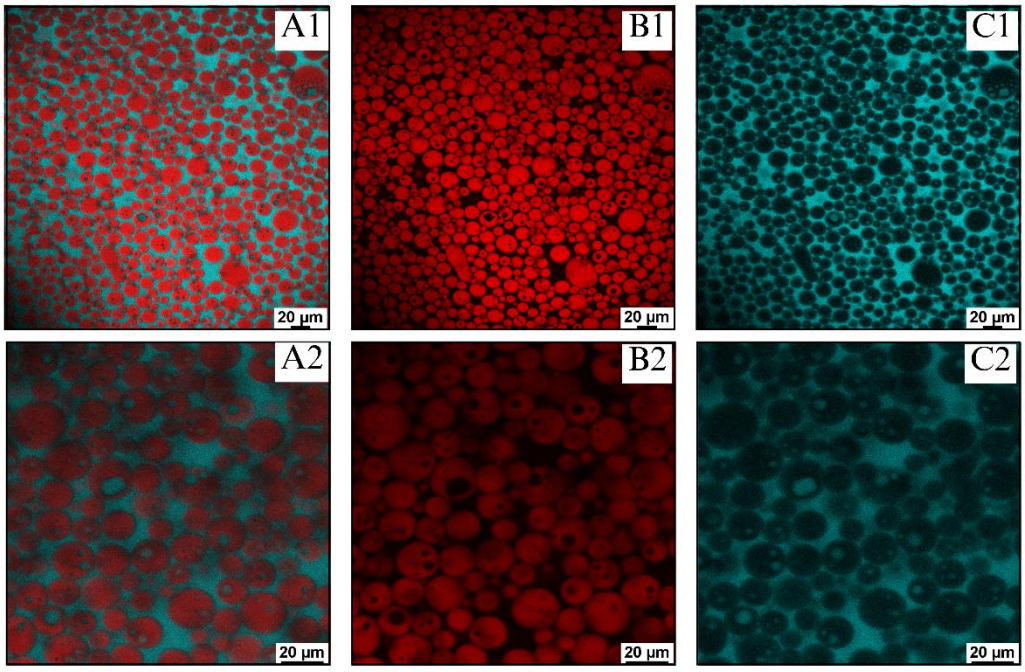

Figure A 1 - Confocal microscopy images of emulsion stabilized with HA-P with 62.5% oil phase. A1 and A2 show the overlapped images, B1 and B2 show the fluorescence of Nile Red, and C1 and C2 show the autofluorescence of HA-P. Images were made with 40x magnification (A1, B1 and C1) and 60x magnification (A2, B2 and C2).